From the Department of Physiology and Pharmacology
Karolinska Institutet, Stockholm, Sweden

NITRIC OXIDE IN CARDIOVASCULAR AND RENAL DISEASE

Role of Organic Nitrates, Inorganic Nitrate and Red Blood Cells

Zhengbing Zhuge

Karolinska Institutet

Stockholm 2022

NITRIC OXIDE IN CARDIOVASCULAR AND RENAL DISEASE
Role of organic nitrates, inorganic nitrate and red blood cells

THESIS FOR DOCTORAL DEGREE (Ph.D.)

By

Zhengbing Zhuge

The thesis will be defended in public at Karolinska Institutet, Biomedicum, Lecture Hall Eva & Georg Klein (D0320), Solna, 25th of February

Principal Supervisor:
Associate Prof. Mattias Carlström
Karolinska Institutet
Department of Physiology and Pharmacology

Co-supervisor(s):
Prof. Eddie Weitzberg
Karolinska Institutet
Department of Physiology and Pharmacology

Dr. Marcelo Montenegro
Karolinska Institutet
Department of Physiology and Pharmacology

Prof. Enyin Lai
Zhejiang University, China
Department of Physiology

Prof. A. Erik G. Persson
Uppsala University
Department of Medical Cell Biology

Opponent:
Associate Prof. Malou Friederich Persson
Uppsala University
Department of Medical Cell Biology (MCB)

Examination Board:
Prof. Olof Nylander
Uppsala University
Department of Medical Cell Biology (MCB)

Associate Prof. Ljubica Matic
Karolinska Institutet
Department of Molecular Medicine and Surgery (MMK)

Associate Prof. Mikael Adner
Karolinska Institutet
Institute of Environmental Medicine (IMM)

ABSTRACT

RATIONALE: Cardiovascular and renal disorders are major health problems, which are often co-existing. Mechanistically, these conditions can be attributed to endothelial dysfunction, a process coupled with reduced nitric oxide (NO) bioavailability. In the vasculature, NO is predominantly formed by endothelial NO-synthase (eNOS), which uses L-arginine and oxygen as substrates. Organic nitrates like glyceryl trinitrate (GTN) are clinically used as an exogenous source of NO, with potent vasodilator actions. Despite their long history of use, the undesired side-effects induced by organic nitrates, such as hypotension, headache and development of tolerance, limit their clinical use and demand a need to develop new nitrate preparations. In addition to the classical NOS system, the nitrate-nitrite-NO pathway can serve as additional source of NO generation. Inorganic nitrate is abundant in certain foods, *e.g.* leafy green vegetables and beetroot. Stimulating this NOS-independent system, via the diet, has been linked with favorable cardiovascular, metabolic and renal effects in several disease models. Moreover, the recent discovery of existing NOS in red blood cells (RBCs) has started a debate regarding the role and interaction between RBCs and endothelial NOSs in regulation of vascular function.

AIM: This thesis *I)* characterizes the therapeutic value of restoring NO bioavailability in cardiovascular and renal disease models by using novel organic mononitrate(s) and inorganic nitrate, and *II)* investigates the potential role and interaction between NOS in RBCs and the endothelium in regulation or modulation of vascular function.

METHODS & RESULTS: Combination of *in vivo* disease models, *ex vivo* vessel reactivity as well as *in vitro* studies were used. **Study I-II:** A novel organic nitrate 1,3-bis(hexyloxy)propan-2-yl nitrate (NDHP) was synthesized and functionally characterized. It was found that NDHP-derived NO formation was enzymatically mediated by xanthine oxidoreductase (XOR). Moreover, NDHP treatment in contrast to GTN was not subject to tolerance in isolated small arteries and NDHP attenuated angiotensin II-induced hypertension and endothelial dysfunction in rats. **Study III:** Inorganic nitrate supplementation, increased NO bioactivity, dampened oxidative stress and inflammation and ameliorated mitochondrial abnormalities, which were associated with protection against development of renal ischemia-reperfusion (IR) injuries in mice. This novel approach may have therapeutic value by reducing the risk of acute and chronic kidney disease as well as cardiovascular co-morbidities. **Study IV:** Using *ex vivo* co-incubation of isolated RBCs and aortas from eNOS-deficient and control mice, it was shown that RBCs lacking NOS induced oxidative stress and endothelial dysfunction in healthy vessels. This pathological vascular phenotype could be prevented by inhibition of arginase activity and by scavenging of NADPH oxidase-derived reactive oxygen species.

CONCLUSION: Restoring NO bioactivity, by using novel organic nitrates or inorganic nitrate, is coupled with favorable effects in models of cardiorenal disease. In addition, arginase and oxidative stress is involved in the interaction between NOS in RBCs and the endothelium. Future studies are needed to further characterize underlying mechanisms and to investigate the potential therapeutic value.

LIST OF SCIENTIFIC PAPERS

1. **Synthesis and characterization of a novel organic nitrate NDHP: Role of xanthine oxidoreductase-mediated nitric oxide formation**

   Zhengbing Zhuge, Luciano L Paulo, Arghavan Jahandideh, Maria C R Brandão, Petrônio F Athayde-Filho, Jon O Lundberg, Valdir A Braga, Mattias Carlström, Marcelo F Montenegro

   Redox Biology. 2017 Oct; 13:163-169.

2. **The novel organic mononitrate NDHP attenuates hypertension and endothelial dysfunction in hypertensive rats**

   Luciano L. Paulo, Josiane Campos Cruz, **Zhengbing Zhuge**, Alynne Carvalho-Galvão, Maria C.R. Brandão, Thiago F. Diniz, Sarah McCann Haworth, Petrônio F. Athayde-Filho, Virginia S. Lemos, Jon O. Lundberg, Marcelo F. Montenegro, Valdir A. Braga, Mattias Carlström

   Redox Biology 2018; 15:182–191

3. **Renovascular effects of inorganic nitrate following ischemia-reperfusion of the kidney**

   Gensheng Zhang*, Huirong Han*, **Zhengbing Zhuge**, Fang Dong, Shan Jiang, Wenwen Wang, Drielle D Guimarães, Tomas A Schiffer, En Yin Lai, Lucas Rannier Ribeiro Antonino Carvalho, Ricardo Barbosa Lucena, Valdir A Braga, Eddie Weitzberg, Jon O Lundberg, Mattias Carlstrom. *Equal contribution*

   Redox Biology. 2021 Feb; 39:101836.

4. **Red blood cells from endothelial nitric oxide synthase-deficient mice induce vascular dysfunction involving oxidative stress and endothelial Arginase I**

   Zhengbing Zhuge*, Sarah McCann Haworth*, Carina Nihlén, Lucas Carvalho, Francesca Leo, Andrei L. Kleschyov, Miriam Cortese-Krott, Eddie Weitzberg, Jon O. Lundberg, Mattias Carlstrom.
   * Equal contribution

   Manuscript

ADDITIONAL PAPERS NOT INCLUDED IN THIS THESIS

1. **Red blood cells from patients with pre-eclampsia induce endothelial dysfunction**

   McCann Haworth SM*, **Zhengbing Zhuge***, Nihlen C, Von Rosen MF, Weitzberg E, Lundberg JO, Krmar RT, Nasiell J and Carlstrom M.

   J Hypertens. 2021;39:1628-1641. *Equal contribution

2. **Head-to-head comparison of inorganic nitrate and metformin in a mouse model of cardiometabolic disease**

   Cordero-Herrera I, Guimaraes DD, Moretti C, **Zhengbing Zhuge**, Han H, McCann Haworth S, Uribe Gonzalez AE, Andersson DC, Weitzberg E, Lundberg JO and Carlstrom M.

   Nitric Oxide. 2020;97:48-56.

3. **Dietary nitrate attenuates high-fat diet-induced obesity via mechanisms involving higher adipocyte respiration and alterations in inflammatory status**

   Peleli M, Ferreira DMS, Tarnawski L, McCann Haworth S, Xuechen L, **Zhengbing Zhuge**, Newton PT, Massart J, Chagin AS, Olofsson PS, Ruas JL, Weitzberg E, Lundberg JO and Carlstrom M

   Redox Biol. 2020;28:101387

4. **AMP-activated protein kinase activation and NADPH oxidase inhibition by inorganic nitrate and nitrite prevent liver steatosis**

   Cordero-Herrera I, Kozyra M, **Zhengbing Zhuge**, McCann Haworth S, Moretti C, Peleli M, Caldeira-Dias M, Jahandideh A, Huirong H, Cruz JC, Kleschyov AL, Montenegro MF, Ingelman-Sundberg M, Weitzberg E, Lundberg JO and Carlstrom M

   Proc Natl Acad Sci U S A. 2019;116:217-226.

5. **Hemoglobin beta93 cysteine is not required for export of nitric oxide bioactivity from the red blood cell**

   Sun CW, Yang J, Kleschyov AL, **Zhengbing Zhuge**, Carlstrom M, Pernow J, Wajih N, Isbell TS, Oh JY, Cabrales P, Tsai AG, Townes T, Kim-Shapiro DB, Patel RP and Lundberg JO.

   Circulation. 2019;139:2654-2663.

6. **Dietary nitrate reduces blood pressure in rats with angiotensin II-induced hypertension via mechanisms that involve reduction of sympathetic hyperactivity**

   Guimaraes DD, Cruz JC, Carvalho-Galvao A, **Zhengbing Zhuge**, Marques SM, Naves LM, Persson AEG, Weitzberg E, Lundberg JO, Balarini CM, Pedrino GR, Braga VA and Carlstrom M

   Hypertension. 2019;73:839-848.

7. **The obligatory role of host microbiota in bioactivation of dietary nitrate**

   Moretti C, **Zhengbing Zhuge**, Zhang G, Haworth SM, Paulo LL, Guimaraes DD, Cruz JC, Montenegro MF, Cordero-Herrera I, Braga VA, Weitzberg E, Carlstrom M and Lundberg JO

   Free Radic Biol Med. 2019;145:342-348.

8. **Extravasal albumin concentration modulates contractile responses of renal afferent arterioles**

   Gao X, Liu ZZ, Mohammed H, Braun D, **Zhengbing Zhuge**, Liu M, Lai EY, Jansson L, Carlstrom M, Patzak A and Persson AEG

   Acta Physiol (Oxf). 2018;222.

9. **Enhanced renal afferent arteriolar reactive oxygen species and contractility to endothelin-1 are associated with canonical Wnt signaling in diabetic mice**

   Zhang S, Huang Q, Wang Q, Wang Q, Cao X, Zhao L, Xu N, **Zhengbing Zhuge**, Mao J, Fu X, Liu R, Wilcox CS, Patzak A, Li L and Lai EY

   Kidney Blood Press Res. 2018;43:860-871.

10. **Blood pressure-lowering effect of orally ingested nitrite is abolished by a proton pump inhibitor**

    Montenegro MF, Sundqvist ML, Larsen FJ, **Zhengbing Zhuge**, Carlstrom M, Weitzberg E and Lundberg JO

    Hypertension. 2017;69:23-31.

11. **Renal denervation attenuates hypertension and renal dysfunction in a model of cardiovascular and renal disease, which is associated with reduced NADPH and xanthine oxidase activity**

    Peleli M, Flacker P, **Zhengbing Zhuge**, Gomez C, Wheelock CE, Persson AEG and Carlstrom M

    Redox Biol. 2017;13:522-527.

12. **Dietary nitrate attenuates renal ischemia-reperfusion injuries by modulation of immune responses and reduction of oxidative stress**

    Yang T, Zhang XM, Tarnawski L, Peleli M, **Zhengbing Zhuge**, Terrando N, Harris RA, Olofsson PS, Larsson E, Persson AEG, Lundberg JO, Weitzberg E and Carlstrom M

    Redox Biol. 2017;13:320-330.

13. **Genetic abrogation of adenosine A3 receptor prevents uninephrectomy and high Salt-induced hypertension**

    Yang T, Zollbrecht C, Winerdal ME, **Zhengbing Zhuge**, Zhang XM, Terrando N, Checa A, Sallstrom J, Wheelock CE, Winqvist O, Harris RA, Larsson E, Persson AE, Fredholm BB and Carlstrom M

    J Am Heart Assoc. 2016;5.

CONTENT

LIST OF ABBREVIATIONS

2K1C	two-kidney one-clip
Ach	acetylcholine
AKI	acute kidney injury
Ang II	angiotensin II
Arg1	arginase 1
BH_4	tetrahydrobiopterin
BUN	blood urea nitrogen
cGMP	cyclic guanosine monophosphate
CKD	chronic kidney disease
CVD	cardiovascular disease
DAF-2 DA	4,5-diaminofluorescein diacetate
DAPI	4',6-diamidino-2-phenylindole
DBA	2,3-dihydroxybenzaldehyde
DHE	dihydroethidium
DMEM	Dulbecco's modified eagle's medium
DPBS	Dulbecco's phosphate-buffered saline
EDRF	endothelium-derived relaxing factor
eNOS	endothelial NOS
EDR	endothelial-dependent relaxation
EIR	endothelial-independent relaxation
Emax	maximum relaxation effect
EPR	electron paramagnetic resonance
GEC	glomerular endothelial cell
GFR	glomerular filtration rate
GTN	glyceryl trinitrate
H_2O_2	hydrogen peroxide
H&E	hematoxylin-eosin
HDX	hydroxocobalamin
HOCl	hypochlorous acid
IBMX	3-Isobutyl-1methylxanthine
iNOS	inducible NOS
IR	ischemia-reperfusion
I.V.	intravenous

KCl	potassium chloride
KO	knock-out
L-NAME	L-NG-Nitroarginine Methyl Ester
L-NNA	N-omega-Nitro-L-arginine
mtALDH	mitochondrial aldehyde dehydrogenase
MAP	mean arterial pressure
NADPH	nicotinamide-adenine dinucleotide phosphate
$NaNO_3$	sodium nitrate
NDHP	1,3-bis(hexyloxy)propan-2-yl nitrate
nNOS	neuronal NOS
NO	nitric oxide
NO_2^-	nitrite
NO_3^-	nitrate
NOS	nitric oxide synthase
NOX	NADPH oxidase
$O_2^{\cdot-}$	superoxide anion
ODQ	[1,2,4]oxadiazolo[4,3-a]quinoxalin-1-one
$\cdot OH$	hydroxyl radical
$ONOO^-$	peroxynitrite
PAS	periodic acid schiff
PDE	phosphodiesterase
PETN	pentaerythritol tetranitrate
PHE	phenylephrine
PTIO	2-phenyl-4,4,5,5-tetramethylimidazoline-1-oxyl 3-oxide
PSS	physiological salt solution
RAS	renin-angiotensin system
$ROO^{\cdot}$	peroxyl radical
RBC	red blood cell
ROS	reactive oxygen species
sGC	soluble guanylyl cyclase
SIN-1	linsidomine
SNP	sodium nitroprusside
TFAM	mitochondrial transcription factor A
XO	xanthine oxidase
XOR	xanthine oxidoreductase

1 INTRODUCTION

1.1 Cardiovascular disease and vascular dysfunction

Cardiovascular disorders including hypertension, coronary heart disease and cerebrovascular disease are major causes of morbidity and mortality worldwide. Epidemiological data from WHO show that more than 1.5 billion people suffer from cardiovascular diseases (CVDs) and associated mortality each year is approximately 18 million, which is more than one third of all deaths worldwide (WHO, 2021). The major causes of death among patients with CVD are myocardial infarction and stroke, accounting for approximately 85% of all cases (WHO, 2021). Vascular dysfunction, including both macro- and microvascular abnormalities, is considered to be an important part of many ageing-associated diseases such as stroke, heart failure, hypertension, renal disease and metabolic disorders [1-7] **(Figure 1)**.
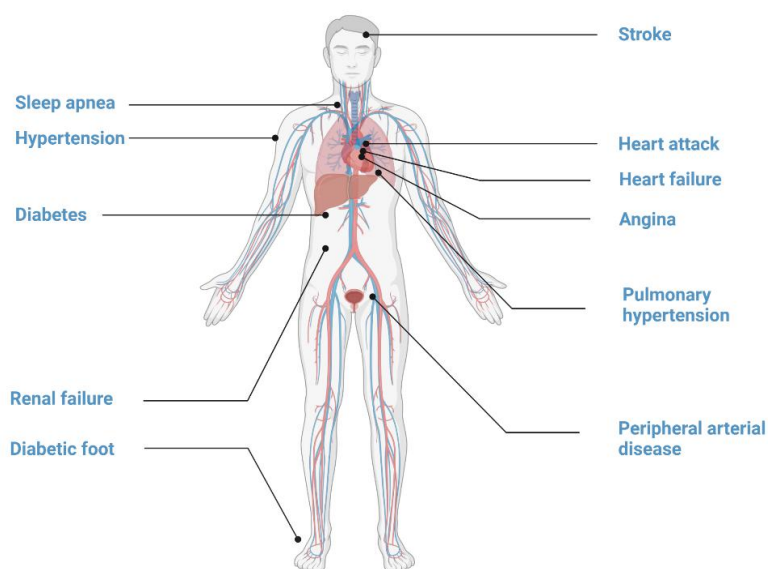
Figure 1. *Vascular dysfunction is considered the precursor of many diseases including cardiovascular diseases such as hypertension, heart failure and peripheral arterial disease, renal diseases such as acute/chronic kidney failure and glomerular disease, as well as metabolic disorders such as diabetes.*

The endothelium, or endothelial system, is one of the largest organs in human body and is composed of up to 10^{12} cells, and weigh more than 1 kg for a 70 kg person [8]. Some researchers even consider this inner layer of the vasculature as an organ in its own right. The endothelium interplays with almost every system in the body, and abnormal function has been implicated in end stage diseases of multiple organ systems including the heart, kidney, liver and the brain **(Figure 1)**. The first and foremost function of the endothelium is the maintenance of vessel wall permeability and regulation of blood flow and organ perfusion. Additionally, normal endothelial cell function is also of great importance for angiogenesis, wound healing processes, and vascular

smooth muscle cell proliferation, as well as modulation of inflammation and fibrosis. In the endothelium, a multitude of important substances are generated in order to uphold vascular homeostasis. We and many other research groups have been focusing on nitric oxide (NO), a small gaseous mediator involved in vasodilation and anti-aggregation of platelets and leukocytes to the endothelium. The importance of the vascular endothelium in regulation of vascular tone was first suggested in 1980 by Furchgott & Zawadski [9]. In *ex vivo* vascular myograph experiments they showed that the vasodilatory action of acetylcholine was abolished when the endothelium was damaged or removed. They suggested that there must be an endothelium-derived relaxing factor (EDRF) conveying the effects of acetylcholine [9]. This discovery started an intense activity to identify EDRF and some years later several additional key observations demonstrated that EDRF was, indeed NO [10, 11]. In 1998 Robert Furchgott, Ferid Murad and Louis Ignarro received the Nobel Prize in Physiology or Medicine "for their discoveries concerning NO as a signaling molecule in the cardiovascular system".

1.2 NO and NO synthases

Numerous studies have demonstrated that NO is central player in the regulation of several organ systems and of particular importance for maintaining cardiovascular homeostasis [12, 13] as well as modulating kidney function [14]. A family of enzymes named NO synthases (NOSs) is generally considered to be the main source of NO generation in the body [15]. There are three different isoforms of NOS: neuronal NOS (nNOS; NOS1), inducible NOS (iNOS; NOS2) and endothelial NOS (eNOS; NOS3), of which both eNOS and nNOS are constitutively expressed proteins [16]. In contrast, iNOS is inducible and activated by inflammatory stimuli and plays a role in host defense [17]. eNOS is mainly located to the vascular endothelium, and NO derived from this particular NOS isoform is generally considered to play a pivotal role in the regulation of vascular tone and organ perfusion, cell proliferation, platelet aggregation and adhesion of leukocytes [16]. In addition, eNOS-derived NO production and signaling also contributes to several protective effects within the cardiovascular system [16, 18] and in the kidney [14].

Apart from normal ageing and genetic factors, several life-style associated risk factors such as obesity, hypertension, hyperlipidemia, and use of tobacco contribute to the initiation and progression of endothelial dysfunction with compromised eNOS function [8, 19]. Visceral obesity is considered one of the major life-style-associated cardiovascular risk factor and is closely coupled with physical inactivity and unhealthy dietary habits [20]. Another important cause of reduced NO bioavailability and signaling is oxidative stress in the vasculature [14, 21].

1.3 Oxidative stress and endothelial dysfunction

Reactive oxygen species (ROS) are generated from molecular oxygen by cells during normal metabolism of sugars, nucleic acids, lipids, and proteins but can also be the result of environmental stress factors such as air pollution and smoking tobacco [22]. Under normal

conditions when there is a balance between generation of ROS and antioxidant capacity, ROS have an important signaling function in the cellular machinery. However, oxidative stress is defined as an imbalance between the production of ROS and the capacity of the antioxidant defense systems (e.g. superoxide dismutase, catalase and glutathione) [23]. ROS are very reactive molecules, and during oxidative stress they can damage the cell. ROS can be divided into free radicals and non-radicals, depending if the molecule contains unpaired electrons, making them reactive or not. The major endogenous species are the superoxide anion ($O_2^{\bullet-}$), hydroxyl radical ($^\bullet OH$), hydrogen peroxide (H_2O_2), peroxyl radical ($ROO^\bullet$), hypochlorous acid (HOCl) and peroxynitrite ($ONOO^-$) [23]. Together with mitochondrial electron transport chain, the major enzymatic ROS generating systems in the vasculature are nicotinamide-adenine dinucleotide phosphate (NADPH) oxidase and xanthine oxidase (XO) as well as uncoupled eNOS [24](**Figure 2**). Excessive production of ROS may also contribute to oxidative stress by impairing the function of endogenous antioxidant systems, thus leading to a vicious cycle [24]. Moreover, superoxide can directly reduce NO bioactivity [25] by fast reaction between the molecules leading to formation of the highly reactive species peroxynitrite ($O_2^{\bullet-} + NO \rightarrow ONOO^-$), which may target and damage several biological structures and cellular components [24].
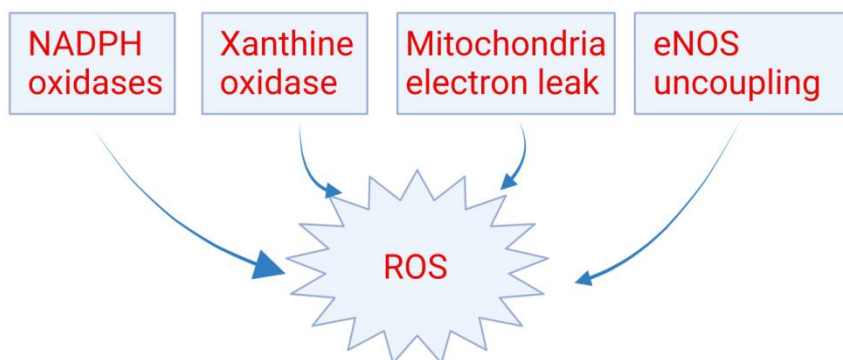
Figure. 2 *Major endogenous sources of ROS in the vasculature. Apart from mitochondrial electron transport chain, ROS can be also enzymatic generated from nicotinamide-adenine dinucleotide phosphate (NADPH) oxidase and xanthine oxidase (XO) as well as uncoupled eNOS in the vasculature. The major ROS include superoxide anion ($O_2^{\bullet-}$), hydroxyl radical ($^\bullet OH$), hydrogen peroxide (H_2O_2), peroxyl radical ($ROO^\bullet$), hypochlorous acid (HOCl) and peroxynitrite ($ONOO^-$).*

It is generally accepted that oxidative stress in the vasculature contributes to the development or the progression of many pathological conditions, including CVDs (e.g. atherosclerosis, hypertension), metabolic disorders including type 2 diabetes, renal disease, and organ ischemia-reperfusion (IR) injuries. Several lines of evidence from both experimental and clinical studies show a link between excessive ROS generation and endothelial dysfunction, associated with hypertension and renal disease [26-28]. The mechanisms contributing to oxidative stress-induced endothelium dysfunction and progression of the disease are likely multifactorial, but may be coupled to compromised NO signaling, increased activity of the renin-angiotensin system (RAS), vascular remodeling, platelet aggregation, reduced vasodilatory and increased vasocontractile

responses, as well as immune cell activation [25, 29, 30]. Future approaches, both nutritional and pharmacological, which dampen excessive ROS generation and increase NO bioavailability, may have therapeutic implications in several disorders including cardiovascular and kidney diseases [14, 21, 31, 32].

1.4 Organic nitrates and NO in cardiovascular disease

Organic nitrates are a class of substances that have a very long tradition in clinical practice to treat chronic heart failure and to bring relief in patients with ischemic heart disease [33]. Despite their widespread use, the mechanisms underlying their vasodilatory effects were unknown for over 100 years and not resolved until the 1970ies. In 1977 Murad and coworkers could show that glyceryl trinitrate (GTN), the archetypical organic nitrate, induced vasodilation by activation of soluble guanylyl cyclase (sGC), which was coupled to an increase in cyclic guanosine monophosphate (cGMP) [34]. The authors suggested that activation might be due to formation of NO since NO alone also increased sGC activity [34]. The coupling of these findings together with the discoveries of EDRF, described above, constituted a major leap in our understanding of vascular physiology. Research during the last decades has revealed the mechanisms of GTN bioactivation and has also shown that the organic nitrates represent a group of substances that are more heterogenous than previously known. Stamler and coworkers could show that mitochondrial aldehyde dehydrogenase (mtALDH) enzymatically convert GTN to 1,2-glyceryldinitrate and nitrite [35]. In this process nitrite is an obligate intermediate in generating NO and they suggested that attenuated biotransformation of GTN by mtALDH underlies the know tolerance to GTN. However, how nitrite is reduced to bioactive NO is still not settled. Some studies have challenged the dogma that the vasodilation by organic nitrates is solely due to NO and other candidates have been suggested, including S-nitroso species and iron-nitrosyl. Interestingly, generation of NO from GTN can also be catalyzed by xanthine oxidoreductase (XOR) [36, 37], an enzyme involved in NO generation from the inorganic anions nitrate and nitrite, discussed below.

Vasodilation of the venous circulations is considered the main target underlying the beneficial effects of organic nitrates in angina pectoris, leading to reduced preload and cardiac wall tension thereby reducing myocardial workload and oxygen demand [33]. At higher doses also arterial vasodilation occurs, including coronary arteries, resulting in reduced cardiac afterload as well as increased myocardial oxygen supply. However, arterial vasodilation also underlies some side effects including hypotension and headache [33, 38].

The fact that organic nitrates are subjected to tolerance has been known for a long time, but the underlying reasons are complex and most likely involve several different mechanisms [38]. Depletion of thiol stores, counteracting neurohormonal vasoconstrictor systems (pseudo tolerance) and increased catecholamine sensitivity, increased activity of phosphodiesterases

(PDEs), desensitization of sGC, GTN-induced oxidative stress and increased endothelin expression are among the candidate mechanisms explaining tolerance [39].

Another negative feature concerning most organic nitrates is their ability to induce endothelial dysfunction [38, 39]. This has been repeatedly shown in animal and human studies, displayed as a reduced vasodilatory response to acetylcholine (Ach). Increased oxidative stress induced by organic nitrates has been suggested as the most likely cause [39]. This stress may lead to oxidation of various components involved in NO generation including tetrahydrobioterin (BH_4), sGC and eNOS itself, leading to eNOS uncoupling and further superoxide generation [39].

Since ageing and CVD are coupled with a decrease in endogenous NO bioavailability there is a constant search for pharmaceutical approach(es) to increase NO by development of new NO-donors, including structurally modified organic nitrates [40]. Preferably, such candidates should have a good pharmacokinetics profile and should not give rise to tolerance and endothelial dysfunction.

1.5 Inorganic nitrate and nitrite as sources of NO

Classically, in a complicated five-step oxidation process the NOS isoforms generate NO from molecular oxygen and L-arginine as substrates and NADPH and BH_4 as co-factors [16]. NO is a very short-lived molecule with a biological half-life ($t_{1/2}$) of milliseconds to a few seconds depending on the location and the oxygen concentration [41]. Serial oxidation of the NO molecule leads to the formation of nitrite (NO_2^-) and nitrate anions (NO_3^-). The former has a relatively short half-life in the circulation (i.e. $t_{1/2} \sim 2$ min in plasma and 20 min in plasma for NO_2^-) compared with the latter more stable anion ($t_{1/2} \sim 5\text{-}8$ hours for NO_3^-) [41, 42]. These anions were previously considered as more or less inert end-products of NO metabolism, but research during the last two decades have demonstrated that they may undergo serial reductions to form NO and other bioactive nitrogen oxide species [43, 44]. Apart from endogenously generated nitrite and nitrate, via metabolism of NOS-derived NO, the other main source of these anions is the diet. Green leafy vegetables and beetroot are especially high in nitrate, that after ingestion is very rapidly and efficiently (~100%) absorbed in the gut [45, 46]. For nitrate to be a source of the formation of bioactive nitrogen species including NO it has to be presented to bacteria which contain efficient nitrate reductases, a function much less pronounced in mammalian cells [47]. Irrespective of its source of generation, either enzymatically from the NOSs or from the diet, circulating nitrate is actively taken up by the salivary glands and excreted into the oral cavity where commensal bacteria reduce nitrate to nitrite [47, 48]. Hence, saliva at any given timepoint is 10-100 higher than plasma in nitrate and nitrite. Salivary nitrite is swallowed and in the acidic stomach parts of the nitrite is immediately reduced to NO (with several local effects, described in [49]), while the majority passes down to the gut and is absorbed. In the circulation and in tissues there are several enzymatic and non-enzymatic pathways for nitrite reduction to NO and other reactive nitrogen intermediates, including XOR, deoxyhemoglobin, deoxymyoglobin and aldehyde oxidase [50-55]. The described enterosalivary

circulation of nitrate is crucial for nitrate to be able to be bioactivated to nitrite and NO (**Figure 3**). This differs from the classical NOS-NO pathway since it is potentiated in states of hypoxia and ischemia, conditions where the NOSs are malfunctional [56-58]. Even if the NO_3^-- NO_2^-- NO pathway works also during normoxia it may be considered as a protective backup system that is potentiated in situations with poor perfusion. The dietary aspects are interesting since there is possibility to boost NO levels in the body by certain food components rich in nitrate.
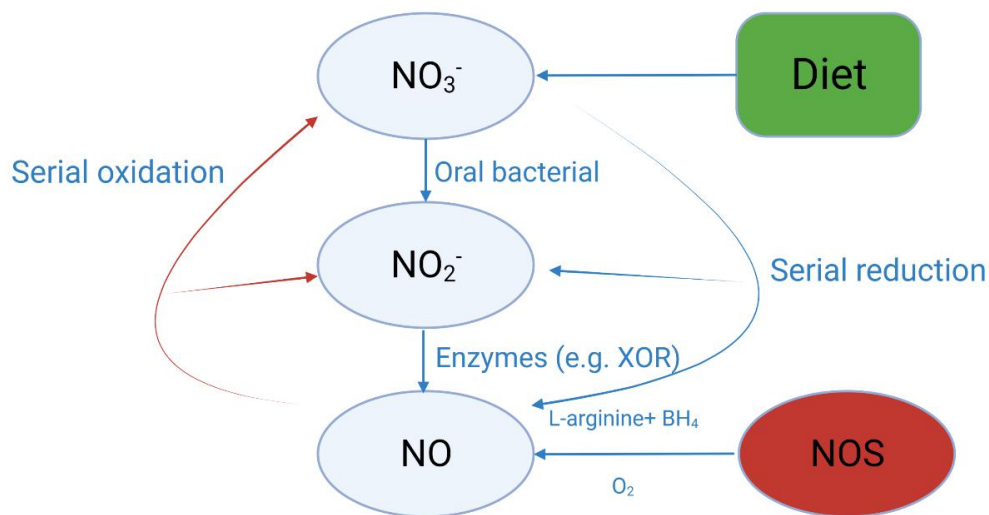

Figure 3. *Pathways for endogenous NO generation and metabolism - Role of the NOS system and the nitrate-nitrite-NO pathway. The NOS isoforms generate NO after a five-step oxidation process from molecular oxygen and L-arginine as substrates and NADPH and BH4 as co-factors. Serial oxidation of NO leads to the formation of nitrite (NO_2^-) and nitrate anions (NO_3^-). Nitrate-nitrite-NO pathway: the bioactivation of nitrate from dietary or endogenous sources starts with reduction to nitrite by oral commensal bacteria followed by further reduction to bioactive NO via different enzymatic and non-enzymatic pathways, involving xanthine oxidoreductase, deoxyhemoglobin, deoxymyoglobin and aldehyde oxidase.*

1.6 Supplementation of inorganic nitrate and nitrite in cardiovascular and renal disease

Today several experimental and clinical studies have shown that dietary supplementation with nitrate and nitrite is associated with favorable cardiovascular effects (e.g. lowering of blood pressure, improved flow-mediated dilatation, attenuated platelet aggregation) [12, 40]. A recent meta-analysis of several clinical studies concluded that the blood pressure lowering effect of daily nitrate supplementation (5-10 mmol/day) for 1-6 weeks was -4.1 and -2.0 mmHg for systolic and diastolic pressure, respectively [59]. Experimental studies have showed that nitrite treatment may ameliorate ischemia-reperfusion (IR) injuries of the heart [60, 61] In addition, it has been shown that dietary nitrate supplementation exerts positive effects in experimental models of metabolic disorders including type 2 diabetes and associated CVD [62].

Several experimental studies, but limited clinical trials, have showed that dietary supplementation with nitrate or acute treatment with nitrite can influence renal perfusion and glomerular filtration as well as tubular reabsorption [14, 21]. These approaches have been associated with renal protection in experimental models of cardiorenal disease associated with oxidative stress and compromised NOS function [21]. Renal ischemia-reperfusion (IR) injury is a common cause of acute kidney injury (AKI) in clinical scenarios such as circulatory chock, kidney transplantation and cardiac bypass surgery. This condition is associated with increased risk of developing chronic kidney disease (CKD) and CVD, which involves oxidative stress, compromised NO signaling and endothelial dysfunction [14, 21]. We recently showed that dietary pretreatment with nitrate counteracted subsequent renal IR injury [63]. However, less is known about the potential therapeutic value of stimulating the nitrate-nitrite-NO pathway in connection with IR and AKI in order to reduce the risk of developing CKD and CVD.

1.7 Mechanism(s) contributing to the effects of inorganic nitrate and nitrite therapy

The mechanisms contributing to the beneficial effects of nitrate and nitrite on cardiovascular, renal and metabolic health are considered multifactorial, and commensal bacteria together with several organ systems are involved in the bioactivation of these anions [12, 14, 62, 64]. In addition to generation of NO and other bioactive nitrogen oxide species, which directly can influence organ functions, several studies have concluded that treatment with inorganic nitrate and nitrite can reduce oxidative stress [63, 65-67]. The mechanisms contributing to such effect is primarily considered to be attenuation of NADPH oxidase-derived superoxide and XOR-derived hydrogen peroxide, but modulation of ROS generated from the electron transport chain of the mitochondria and from uncoupled eNOS have also been proposed [12, 14, 62]. These dampening effects of the nitrate-nitrite-NO pathway on ROS production and oxidative stress may all be associated with favorable effects on the cardiovascular and renal systems.

1.8 Functional eNOS in RBCs and its role on regulating vascular homeostasis

The contribution of NO in the circulation has largely been attributed to eNOS in the vascular endothelium. In 2006, Kleinbongard *et al.* firstly proposed an active and functional eNOS in human RBCs which localized to the plasma membrane and the cytoplasm of RBCs [68]. Initially, this finding was met with skepticism as few authors believed any appreciable amounts of NO could be formed in the RBC without being rapidly scavenged by the abundant hemoglobin. Later publications, however, indicated possible physiological activities of RBCs-eNOS, including inhibition of platelet activation and regulation of RBC membrane deformability. Today, the exact role(s) of RBC-eNOS in regulation of cardiovascular homeostasis are still being debated [69]. Yang and colleagues found that arginase in RBCs regulates RBC-eNOS activity and export of cardioprotective NO bioactivity [70]. Similar findings also support a potential role of shear stress and exercise training on RBC signaling and function, and a role of RBC-eNOS mediated

cardiovascular protection [71-74]. Moreover, Leo *et al.* recently suggested that RBC-eNOS independently regulates circulating NO metabolites and blood pressure in addition to endothelium-eNOS [75]. Possible role of RBC-eNOS and export of NO bioactivity is shown in **Figure 4.**
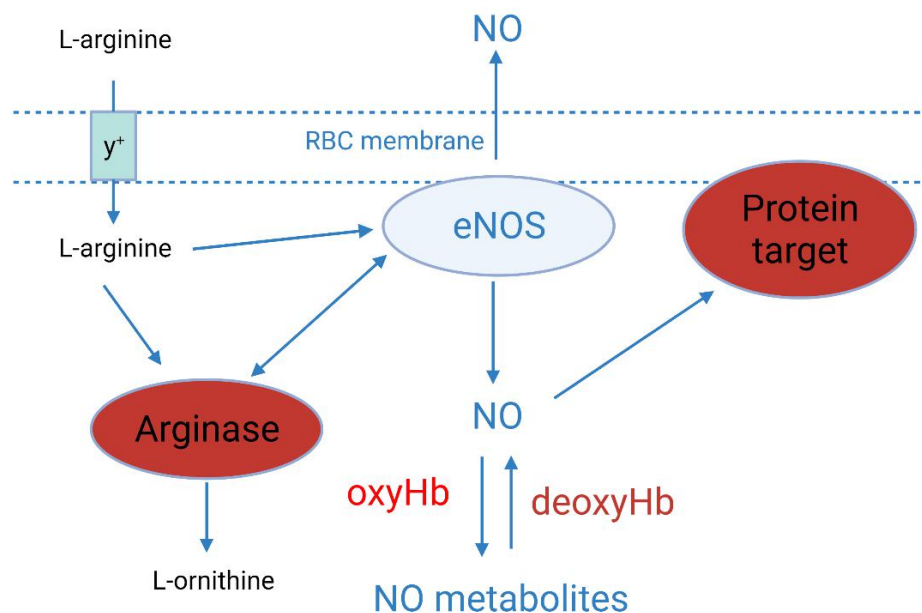

Figure 4. *Possible signaling and formation of RBC eNOS-derived NO and interactions with other RBC enzymes. Extracellular L-arginine can be transported to RBCs via y+ cationic amino acid transporter. In RBCs, L-arginine is the common substrate for arginase and eNOS. Arginase catalyzes the conversion of L-arginine to L-ornithine and urea, whereas eNOS converts L-arginine to form L-citrulline and NO, which is metabolized by oxyhemoglobin (oxyHb) and oxygen to nitrite and nitrate. The NO metabolite nitrite can be reduced back to bioactive NO via different mechanism(s) including the action of deoxyhemoglobin (deoxyHb).*

In addition, recent evidence also indicated that RBC arginase-1 (Arg1) tightly regulates RBC eNOS-derived NO bioactivity [70]. This has been shown in RBCs from type 2 diabetic [76-78] and pre-eclamptic patients [79] *ex vivo,* which in turn may influence endothelium function in a negative way. Although studies thus far have highlighted the link between dysregulation of RBC homeostasis and cardiometabolic pathologies *per se*, mechanistic knowledge of the specific functional interaction between RBC eNOS and the vascular endothelium is still lacking. More laboratory experiments are therefore needed to clarify the underlying mechanisms, and to further investigate the potential clinical importance of targeting/modulating the proposed interaction between RBC eNOS and the vascular endothelium.

2 RESEARCH AIMS

The overall aim of this thesis was to *I)* investigate the therapeutic value of increasing NO formation and signaling in models of cardiovascular and renal disease by using a novel organic mononitrate and inorganic nitrate, and to *II)* further investigate the significance of RBC eNOS in modulation of vascular endothelial homeostasis. Below, the **specific aims** for the studies in this thesis are described:

STUDY I: To synthesize and characterize the novel organic mononitrate; 1,3-bis(hexyloxy)propan-2-yl nitrate (NDHP).

STUDY II: To characterize the NO donating and vasodilatory properties of NDHP, and to investigate the acute and the chronic cardiovascular effects of NDHP treatment in experimental models of hypertension.

STUDY III: To investigate the therapeutic value of boosting the nitrate-nitrite-NO pathway during development of IR-induced renal and cardiovascular dysfunction.

STUDY IV: To investigate the potential role and interaction between eNOS in RBCs and the endothelium in regulation of vascular function.

3 MATERIALS AND METHODS

Brief description of the methods used in this thesis are described below. For more detailed information, please see the materials and methods sections of each scientific paper.

3.1 Synthesis of NDHP

For detailed information about the synthesis of NDHP, which was carried out by colleagues at Biotechnology Center, Federal University of Paraíba, João Pessoa, PB, Brazil, please refer to material and methods section in Paper I (Zhuge et al. *Redox Biology*. 2017 Oct; 13:163-169)

3.2 Animals and surgical protocols

In study I and study II, both male and female (200-250g) Wistar rats were housed in a temperature-controlled room with a 12-h light/dark cycle and given standard rodent chow and tap water ad libitum. The renovascular hypertension model (2K1C) used in study II, was induced by clamping the right renal artery. During ketamine/xylazine anesthesia (75 and 10 mg/kg, i.p., respectively), the animals were subjected to a midline abdominal incision after which a U-shaped silver clip was placed around the right renal artery. Sham operations were performed in the same way with exception of arterial clipping. After surgery the animals remained untouched for six weeks to develop arterial hypertension. In study II, we also used a model of hypertension, induced by L-NAME treatment in combination with angiotensin II (Ang II). Here, blood pressure was recorded with tail-cuff technique during baseline (3 days), thereafter an osmotic minipump was implanted subcutaneously delivering Ang II continuously for at least 14 days, as described previously [80]. At the same time (*i.e.* Day 0), L-NAME treatment was initiated, given via the drinking water (0.5 g/L), and blood pressure was measured again during days 10-14.

In order to study the effects of inorganic nitrate on kidney ischemia-reperfusion in study III, 10-12-week-old male C57BL/6J mice were used. They were given intraperitoneal boluses of either placebo (NaCl) or sodium nitrate ($NaNO_3$, 10 mg/kg) two hours prior to surgery. Under isoflurane anesthesia the mice then underwent surgery where the left kidney was clamped for 45 min. Sham surgeries were performed in the same way, but without clamping. During a 2 week follow up period sodium nitrate (1 mmol/kg/day) or saline were supplemented in the drinking water.

In study IV, male C57BL/6J mice (Janvier Laboratories) and male C57BL/6J eNOS knockout (KO) mice (Jackson Laboratory, USA) were housed in our animal facilities at Karolinska Institutet, with a 12:12 h light/dark cycle. Endothelial cell arginase 1 KO mice (EC Arg 1 KO) were generated and characterized in collaboration with colleagues at University of Düsseldorf, Germany (Cortese-Krott M. *et. al.*). Animals were fed with standard rat chow and water ad libitum. RBCs and vessels were obtained for vascular reactivity studies.

3.3 *In vivo* measurements

3.3.1 Blood pressure monitoring

Blood pressure was measured and recorded using the non-invasive tail-cuff method with the CODA system (Kent Scientific, Torrington, CT, USA) at the end of the 2-week observation period, similar to that described previously ([81]). In brief, animals were conditioned on a warm plate at 37 degrees for 10 min and then placed in plastic restrainers. Animals were trained to the restrainers at least three days before recordings. Values were collected over 3 consecutive days and individual median of all accepted values were used for assessment.

3.4 *Ex vivo* vascular reactivity studies

3.4.1 Vascular reactivity study on isolated mesenteric arteries

In study I and II, a multiwire myograph system (Model 620 M, Danish Myo Technology, Denmark) was used to evaluate the potential vascular effects of NDHP. Briefly, rat mesenteric tissues were placed in cold Tyrode's solution, the superior mesenteric artery was isolated and adhering adipose tissue was carefully removed. Arteries were cut into 2 mm long rings which were mounted in a myograph chamber, connected to a tension transducer (PowerLab™, AD-Instruments, MA, U.S.A.). Rings were stabilized under 0.75g resting tension for 1h. Vessel viability was verified by the presence of a proper contraction to phenylephrine (PHE, 10 μM), and successful removal of the endothelium was verified by the absence of a response to Ach (10 μM). For NDHP concentration-response curve, vessels were pre-constricted with PHE (1 μM) until the plateau was observed, then cumulative dose of NDHP (10^{-12}-10^{-3} mol/L) was added to the chamber.

3.4.2 Induction of tolerance in rat mesenteric artery

In study I, denuded mesenteric artery rings were preincubated with GTN (100 μM) or NDHP (1 mM) for 30 min. To ensure complete removal of the drugs, repeated wash out the rings with physiological solution was performed. The rings were allowed to stabilize for another 60 min with exchange of the chamber solution every 15 min. Contraction was induced with PHE (1 μM) at the end of the stabilization period to reach a plateau, after which cumulative concentrations of GTN (10^{-12}-10^{-3} M) or NDHP (10^{-12}-10^{-3} M) was added to the chamber. The potency (pD2) and maximum relaxation effect (Emax) were calculated. Tolerance of organic nitrates was defined by a compromised relaxation response after preincubation.

3.4.3 Isolation and vessel reactivity of interlobar arteries

In study III, harvested kidneys were kept in ice-cold physiological salt solution (PSS) and used for isolation of the interlobar arteries. Interlobar artery were cut into 2 mm long rings and were mounted on 25 μm tungsten wires in the multi-wire myograph system (Model 620 M, Danish Myo Technology, Denmark). Isometric tension was recorded (Powerlab 4/30, AD Instruments, Australia). Vessels were equilibrated for 20 min and bubbled with carbogen (95% O2; 5% CO2)

at 37 degrees. Viability of the interlobar arteries was accessed by applying with 100 mmol/L KCl, and the presence of endothelium was accessed by response to Ach (more than 70% of relaxation).

3.4.4 Isolation and micro-perfusion of kidney afferent arterioles

In study III, kidneys were removed from anesthetized mice and immediately sliced and as described previously [82-84]. Slices were then placed in ice-cold Dulbecco's modified Eagle's medium (DMEM). A single afferent arteriole with attached glomerulus was micro-dissected and transferred to a temperature-regulated chamber on the stage of an inverted microscope. The glomerulus was fixed with a holding micropipette and the afferent arteriole was cannulated and perfused with a set of micropipettes. The intraluminal pressure of the perfused afferent arteriole was maintained at 60 mmHg during experiments. After a 30 min equilibration period, the diameter of the afferent arteriole was measured in response to cumulative doses of Ang II (10^{-12}-10^{-8} mol/L).

3.4.5 Vascular reactivity study on aortic rings

In study IV, mice aortic rings (2mm) were mounted in the myograph system (Model 620M; Danish Myo Technology, Denmark). PSS-filled chambers were bubbled with carbogen gas and the rings were allowed equilibrate for 45 minutes. A loading force of 6 mN was added to the vessels to mimic near physiological pressure after which KCl (120mM) was applied to access viability. After washing, the aortic rings were pre-constricted with increasing concentrations of PHE (10^{-10}-10^{-5} mol/L) to reach approximately 80% of the KCl-induced contraction. After establishing a stable plateau phase, cumulative concentrations of Ach (10^{-9}-10^{-4} mol/L) were applied. For the endothelium-independent relaxation, a cumulative concentration-dependent response by sodium nitroprusside (SNP, 10^{-9}-10^{-4} mol/L) was induced.

3.5 *In vitro* studies

3.5.1 XOR-mediated NO production from NDHP

In study I, we examined the involvement of XOR in NO formation from NDHP. Briefly, a reactional buffer (PBS pH 7.4) containing purified XOR (0.05 U/mL, Roche), NADH (1 mM, Sigma), and NDHP (1 mM) was used. In certain experiments, NADH was replaced by xanthine (Sigma) or 2,3-dihydroxybenzaldehyde (DBA, Sigma). The reactional buffer was added into an Oxygraph-2k system chamber (Oroboros instruments) at 37 °C. The Oxygraph chamber was connected in line to a chemiluminescence NO analyzer (EcoPhysics, Durnten, Switzerland), using nitrogen gas as carrier (400 mL/min). After an equilibration period, the above mentioned substances were injected into the chamber using Hamilton syringes and real-time NO generation was recorded during one hour. In a subset of experiments, the XOR inhibitor oxypurinol (100 μM), the flavoprotein inhibitor diphenyleneiodonium (DPI) (50 μM), or L-cysteine (5 mM) was added 15 min prior to adding electron donors.

3.5.2 Electron paramagnetic resonance spectroscopy

In study I, XOR dependent NO generation was evaluated by using spin trap based EPR (MiniScope MS400, Magnettech, Germany). The reaction buffer contained XOR (0.05 U/mL), NDHP (1 mM), NADH (1 mM), xanthine (500 μM) or DBA (500 μM). The Dulbecco's phosphate-buffered saline (DPBS) was bubbled over one hour with nitrogen gas to avoid dissolved oxygen. After 5 min of buffer equilibration, the spin trap (Fe(MGD)2) complex was injected using Hamilton syringes and the reaction was allowed for 1 hour. An aliquot was collected using capillary tubes and the spectra were analyzed.

3.5.3 NO measurements by fluorescence microscopy

In study II, indirect measurements of NO generation in mouse mesenteric arteries were performed using fluorescence microscopy and staining with the cell permeable 4,5-diaminofluorescein diacetate probe (DAF-2 DA, Calbiochem, San Diego, CA, USA). In brief, vascular rings were pre-incubated with DAF-2 DA (10 μM) in darkness for 30 mins, fixed in OCT and frozen at -20 °C. Sections were cut (8 μm) and mounted on slides with coverslips. After stimulation the sections were washed and processed. To visualize cell nuclei, 4',6-diamidino-2-phenylindole stain (DAPI) was used. Cytosolic NO levels were assessed by exciting DAF-2 DA at 480 nm using a xenon lamp after which fluorescence was measured at an 515-565 nm. The change in fluorescence intensity, which is calculated as the difference between the final and basal fluorescence indicates NO content (A.U.).

3.5.4 Nitrate, nitrite, cGMP, creatinine, blood urea nitrogen and Ang II levels

In study III plasma levels of nitrite and nitrate were analyzed by HPLC (ENO-20) as described previously [85]. Nitrite and nitrate were separated by reverse phase/ion exchange chromatography followed by nitrate reduction to nitrite by cadmium and reduced copper. Nitrite was derivatized using Griess reagent to form diazo compounds and detected at 540 nm. Plasma used for determination of cGMP was transferred to tubes containing the phosphodiesterase inhibitor, 3-Isobutyl-1methylxanthine (IBMX Sigma-Aldrich #I5879) to inhibit degradation of cGMP and later analyzed with a commercial ELISA kit (GE Healthcare #RPN226).

Creatinine levels in plasma and urine were measured with Creatinine Colorimetric Assay Kits (Cayman Chemical, #700460 and #500701). Creatinine clearance formula (CLCr = UrineCr x Urine flow/PlasmaCr) was used to estimate GFR. The plasma BUN levels were detected by using BUN Colorimetric Detection Kit (Invitrogen, #EIABUN). The levels of Ang II in plasma and kidney tissues were measured by using Ang II ELISA kit (Cloud-Clone Corp., # CEA005Mu). All absorbance readings were done in SpextraMax iD3 (Molecular Devices).

3.5.5 Cell culture using glomerular endothelial cells

In study III, rat glomerular endothelial cells (GECs) (DSMZ ACC262, Germany) were cultured in RPMI 1640 (Gibco) medium with 10% fetal bovine serum and 2 mM L-Glutamine (Gibco), penicillin and streptomycin (50 mg/L, Gibco). Cells were maintained at 37 ∘C in a humidified

atmosphere of 5% CO_2. Hypoxia experiments were performed in 1% oxygen at 37 ∘C for 2 h with the cells incubated in HBSS (Gibco). Cells were pre-incubated with nitrite (10 µM), with or without the XOR inhibitor febuxostat (100 nM), for 30 min before hypoxia. Cell viability was evaluated by PrestoBlue® assay (Invitrogen, A13261 and A13262), and cell mortality was assessed by Trypan Blue exclusion assay (Sigma, T8154-20 ML).

3.5.6 Detection of mitochondrial ROS

In study III, the endothelial cells mentioned above were incubated with a fluorogenic dye (MitoSOXTM, Invitrogen M36008, 2 uM) for 10 min to evaluate mitochondrial superoxide levels. After incubation the cells were washed and the fluorescent signal (SpectraMax iD3 reader, Molecular Devices, USA) was normalized to cell viability.

3.5.7 Arginase activity in RBCs

In study IV, arginase activity was determined via its ability to convert L-Arginine to Urea. Ghost cells from washed murine RBC were prepared using an ice-cold hypotonic buffer (PBS diluted 1:27 in distilled water) to induce opening of membrane pores. The ghosts were then lysed using RIPA buffer with protease inhibitors (Roche). Lysed ghost cells were added to Tris-HCl (50 mM, pH 7.5) containing 10 mM MnCl2. The mixture was activated by heating for 10 min at 56°C. Each sample was incubated at 37°C for 3 h with L-Arginine (50ul of 500 mM Tris HCL at pH 9.7). The reaction was stopped by adding 400 µl of an acid solution (H_2SO_4–H_3PO_4–H_2O=1:3:7). 25 ul of α-isonitrosopropiophenone (9% in ethanol) was added to each sample and standard and the mixture was heated at 100°C for 60 min. The urea concentration was determined at 550 nm using spectrophotometry and calculated as Urea nmol/mg protein/min.

3.6 Histological examination

3.6.1 Hematoxylin-Eosin and Periodic Acid Schiff

In study III, the kidney samples were harvested and fixed in 4% paraformaldehyde solution. Fixed kidney tissues were embedded in paraffin and thereafter sliced and stained with Hematoxylin-Eosin (H&E) or Periodic Acid Schiff (PAS) for histological assessment. Ten randomly chosen fields from each section were captured under 400×magnification. All morphometric analyses were performed in a blinded manner.

3.6.2 TUNEL staining

In Study III, OCT-embedded kidney samples (Tissue-Tek, Torrence, CA, USA) were sliced into 6-µm thick sections and incubated with 20 µg/mL proteinase K for 15 min at room temperature and the Click-iT™ Plus TUNEL Assay (Invitrogen C10618, USA) was used. At the end of the protocol the sections were stained with the DAPI (Invitrogen). Using confocal microscopy, the positive signals were quantified using and were calculated as the ratio of the positive signals to DAPI.

3.6.3 Tissue immunofluorescence staining and confocal microscopy (F4/80)

In study III, frozen kidneys sections (6um) in OCT were prepared and washed with $1 \times$ PBS and blocked with 2% BSA in PBS for 30 min and then incubated with anti-F4/80 (1:50, BIO-RAD Cl:A3-1) overnight and subsequently with a secondary antibody (1:200 Cell signaling Tech #4417), followed by counterstaining with 300 nmol/L DAPI for 3 min. The immunofluorescence signals were visualized under the Zeiss LSM800-Airy confocal microscope.. F4/80 positive signals were quantified using ImageJ/Fiji software and were calculated as the ratio of the positive signals to DAPI.

3.7 Statistical analyses

In general, parametric (normal distribution) and non-parametric (not normal distribution) student t-tests were used to compare differences between two groups/parameters of data. One-way and two-way ANOVA, followed by appropriate post-hoc test (as recommended by the Graph Pad Prism Software (version VIII) were used to compare differences between several groups/parameters. Repeated two-way ANOVA followed by post-hoc analysis was used to compare dose-responses in isolated vessels. Unless otherwise indicated, data presented in this thesis are shown as Mean +/- SEM. A p-value less than 0.05 was considered statistically different.

4 RESULTS AND DISCUSSION

4.1 Study I & II: Synthesis, characterization and cardiovascular effects of the organic mononitrate NDHP

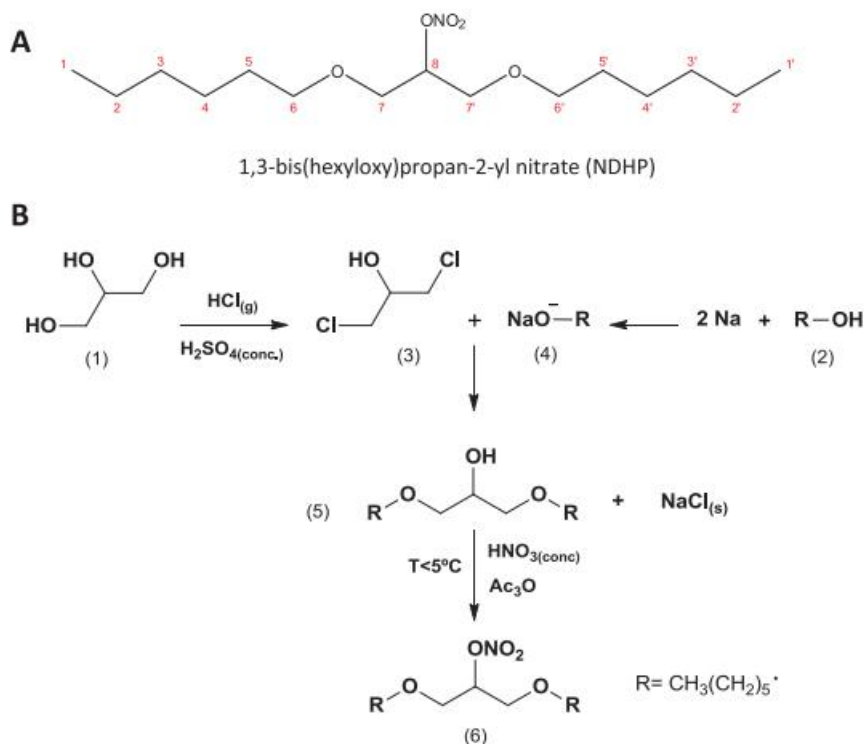### 4.1.1 Structure formulae and synthetic route for NDHP

Figure 5. *Structural formulae (A) and synthesis (B) of 1,3-bis (hexyloxy) propan-2-yl nitrate (NDHP). TLC was used to assess purity of NDHP. The identity and purity of the compound was confirmed by combination of IR, ^{1}H-NMR and ^{13}C NMR spectroscopy. Reaction yield with this approach reached 83.2%.*

4.1.2 Reduction of NDHP to NO: role of XOR

XOR is involved in the final enzymatic step of purine metabolism, but also considered to be a source of ROS. In addition, XOR has been implicated in the bioactivation of inorganic nitrate and nitrite, as well as organic nitrates by mediating NO formation via reduction of these molecules/compounds [36, 37, 86]. In study I and study II, we evaluated if XOR could reduce NHDP to NO by using chemiluminescence detection.

Firstly, in **Figure 6A**, we observed that NDHP alone or in association with XOR was unable to induce NO generation. However, addition of NADH (reduction form of nicotinamide adenine

dinucleotide, NAD$^+$) rapidly induced a robust NO signal, and the effects remained for almost 1 hour following the addition of NADH.

Interestingly, when xanthine was used as the electron donor instead of NADH, no NO generation was, even at higher concentrations of xanthine (**Figure 6B**). On the other hand, under same experimental conditions and using low xanthine concentration (20 μM), we observed a high level of NO generation when inorganic nitrite was added, which could be blocked by the XOR inhibitor oxypurinol (**Figure 6C**). Similar to NADH, using another electron donor, *i.e.* 2,3-dihydroxybenzaldehyde (DBA), also induced a robust NO signal (**Figure 6D**).
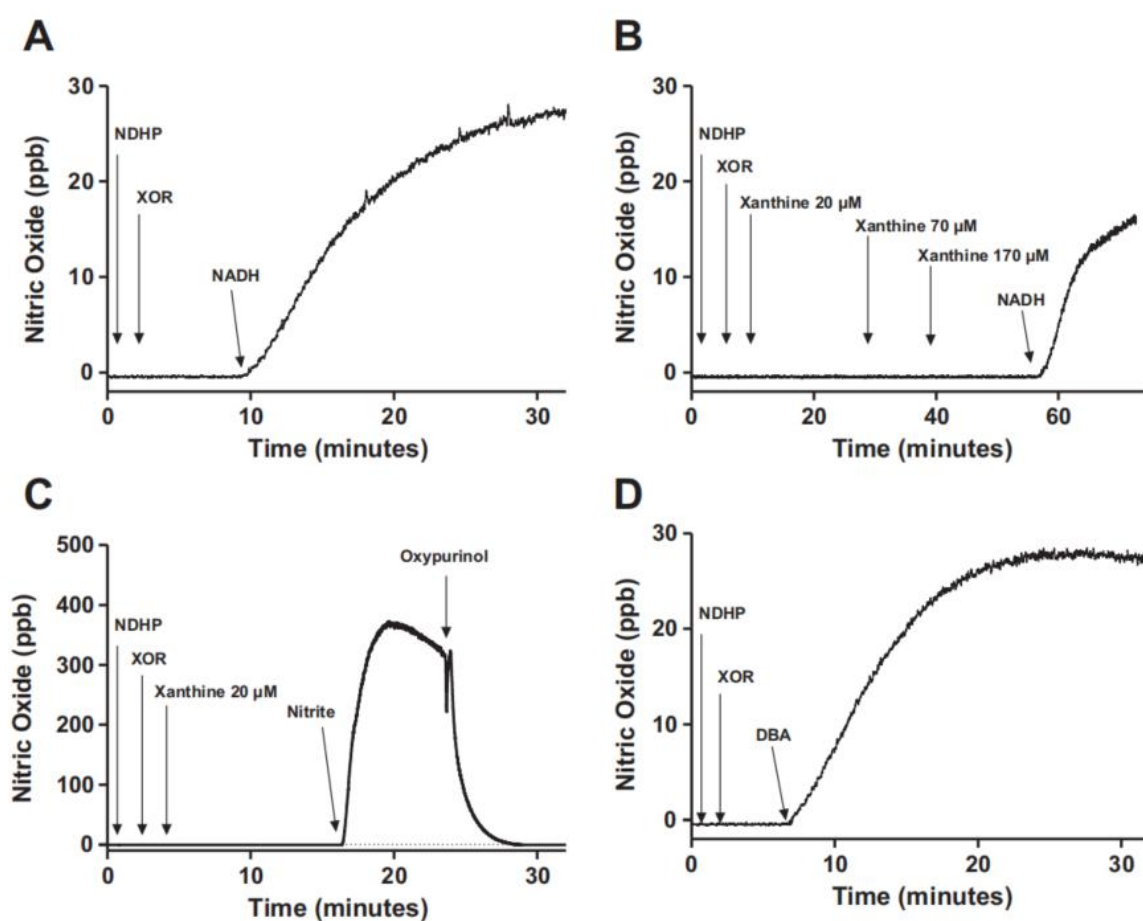

Figure 6. *NDHP-derived NO formation in the presence of XOR and various electron donors. Real-time NO generation was assessed by chemiluminescence in a flow-through system with nitrogen gas as carrier. The tracings are representative of 4-6 independent experiments. For experimental details, please see methods in Paper I.*

These results confirmed that xanthine is not an electron donor for the XOR-mediated bioactivation of NDHP. Finally, we observed that the NDHP-derived NO formation was associated with subsequent accumulation of nitrite and nitrate in the reaction buffer (**Table 1**).

Table 1. *Levels of nitrite and nitrate accumulated in a reaction buffer after incubation with XOR and NDHP.*

NDHP	0.1 mM	1mM	10mM
Nitrite (µM)	7.13 ± 0.52	28.87 ± 4.65	53.70 ± 8.68
Nitrate (µM)	9.33 ± 0.75	26.42 ± 0.84	104.7 ± 9.96

Thiols have been implicated, although debated, in the bioconversion of organic nitrates such as GTN [37]. In our experimental setting, using NADH (1mM) as electron donor, with or without addition of L-cysteine, NO formation was continuously monitored for 1 hour. Based on our findings we could conclude that NDHP-mediated NO formation occurs independent of nitrosothiols (SH-) as an intermediate source.

4.1.3 NDHP-mediated NO signal in resistant arteries is mediated by XOR

Figure 7 and **8** show fluorescence microscopy images of rat mesenteric arteries, and observed changes in fluorescence emitted by DAF-2 DA (used as an index of NO production) in response to various treatments as well as XOR inhibition with febuxostat.

Incubation with DAF-2 DA alone was set at baseline and served as control (Fig 7A & B). Incubation with NDHP significantly increased fluorescence (95.7 ± 3.4 a.u. vs. control 10.9 ± 0.8 a.u., $p < 0.05$). The NO donor linsidomine (SIN-1) served as positive control and increased fluorescence to a similar degree as NDHP (102.5 ± 2.1a.u. vs. control 10.9 ± 0.8 a.u.,$p < 0.05$). The NOS inhibitor N-omega-Nitro-L-arginine (L-NNA), did not affect the increase of fluorescence induced by NDHP or SIN-1 (Fig 7B).

These results suggests that NDHP, similar to the established NO donor SIN-1, generates NO or NO-related species independently of functional NOS.

Changes in the fluorescence emitted by DAF-2 DA after NDHP during simultaneous inhibition of XOR by febuxostat are shown in **Figure 8**. Panel A shows a representative image of incubations with DAF-2 DA alone (control), febuxostat alone, NDHP alone and NDHP + febuxostat. Incubation with NDHP significantly increased the DAF fluorescence and this increment was attenuated by febuxostat, suggesting the involvement of XOR in NDHP-mediated generation of NO species.
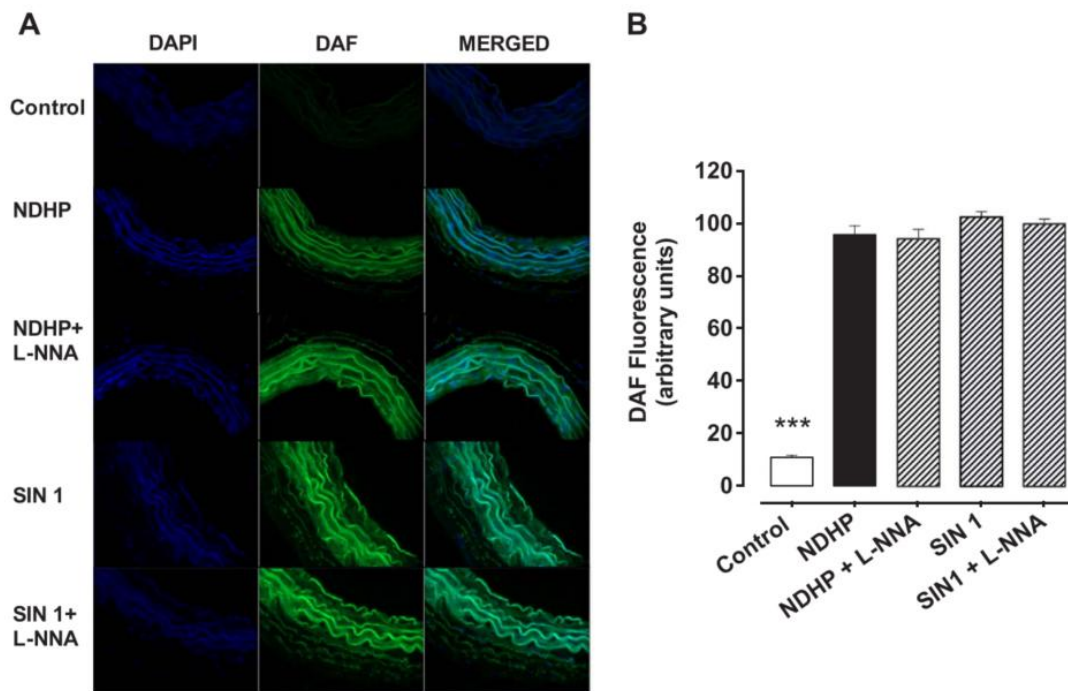
Figure 7. *Imaging of NO and NO related species in rat superior mesenteric arteries. (A) Representative images after incubation with the fluorescent cell permeable probe DAF-2 DA (10 μM). (B) NO production after incubation with DAF-2 DA (control), NDHP, NDHP + L-NNA, Linsidomine (SIN-1) and SIN-1 + L-NNA. *** p<0.001 control versus other treatment groups*
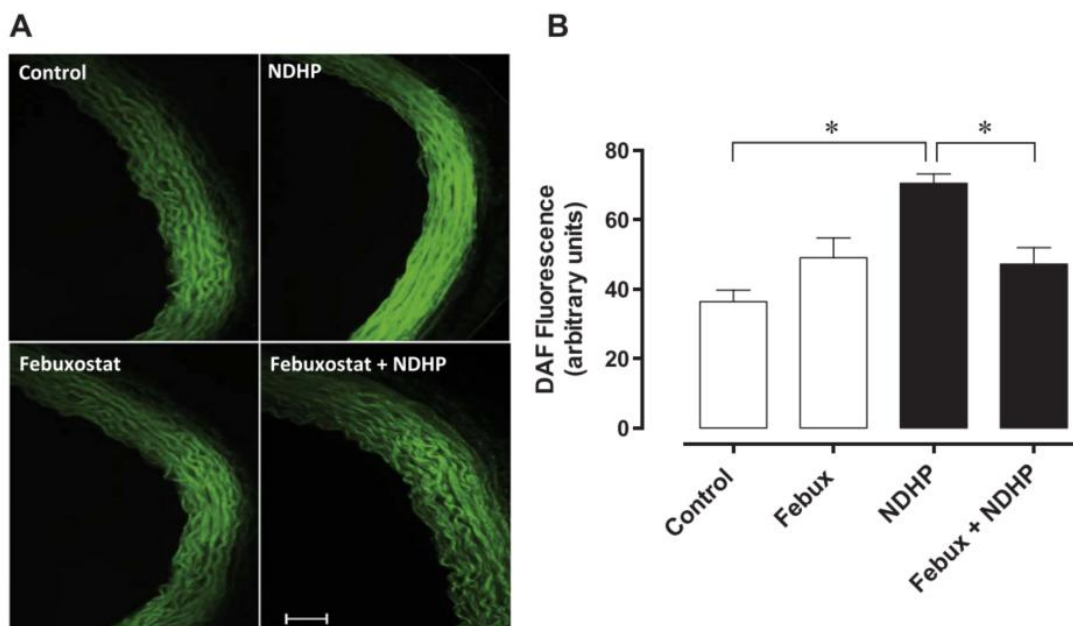

Figure 8. *NDHP-mediated generation of NO species in mesenteric arteries and the involvement of XOR. (A) Representative images of mesenteric artery sections incubated with the DAF-2 DA during different conditions (control, NDHP, febuxostat alone, NDHP + febuxostat). (B) Quantification of DAF fluorescence. * p<0.05 between indicated groups.*

4.1.4 Ex vivo vasorelaxation by NDHP: role of XOR

A concentration-dependent vasorelaxation was observed after adding accumulative NDHP to rat superior mesenteric arteries. The presence or absence of a physically denuded endothelium had no effect on the vasodilatory response to NDHP ($pD2 = 6.3 \pm 0.10$ and $Emax = 92 \pm 7\%$ for intact endothelium; $pD2 = 6.6 \pm 0.07$ and $Emax = 109 \pm 4\%$ for denuded endothelium, $P>0.05$), demonstrating that NDHP-induced vasorelaxation is endothelium-independent (**Figure 9A**). In another set of experiments using mesenteric arteries from mice, we evaluated NDHP-mediated vasorelaxation in the presence of the XOR inhibitor febuxostat and the relaxations were significantly attenuated ($p<0.05$, **Figure 9B**). Together, we confirmed that NDHP-mediated vasorelaxation in small resistant arteries were endothelium-independent and in part dependent of XOR.
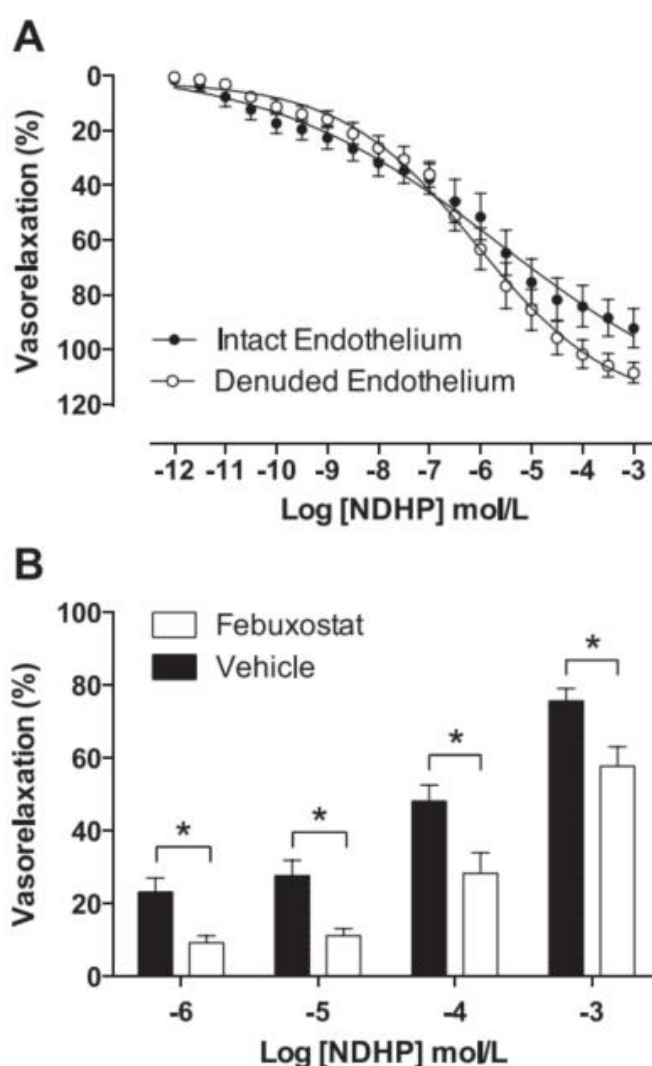

Figure 9. *NDHP-mediated vasorelaxation in both rat and mice mesenteric arteries and the role of XOR. (A) Concentration-response curves of NDHP in rat superior mesenteric arteries and (B) effect of the selective XOR inhibitor febuxostat on vasorelaxation effects of NDHP in mesenteric arteries from mice. No significant differences were found when comparing intact versus denuded-endothelium (P > 0.05, panel A); *p < 0.05 versus vehicle (panel B)*

4.1.5. NDHP-mediated vasorelaxation: modulation of NO bioactivity

In **Figure 10A**, NDHP induced concentration-dependent vasorelaxation in pre-constricted rat mesenteric arteries in the presence of functional endothelium (Emax = 83.3 ± 6.7%). After removal of the endothelium, vasorelaxation was even potentiated (Emax = 113.4 ± 5.3%). Similarly, when vessels were pre-incubated with the NOS-inhibitor L-NG-Nitroarginine Methyl Ester (L-NAME), the NDHP-induced vasorelaxation were increased (Emax = 109.7 ± 1.5% compared with control Emax 83.3 ± 6.7%, **Figure 10B**). This suggests that NOS in the endothelium may dampen NDHP-mediated vasorelaxation.
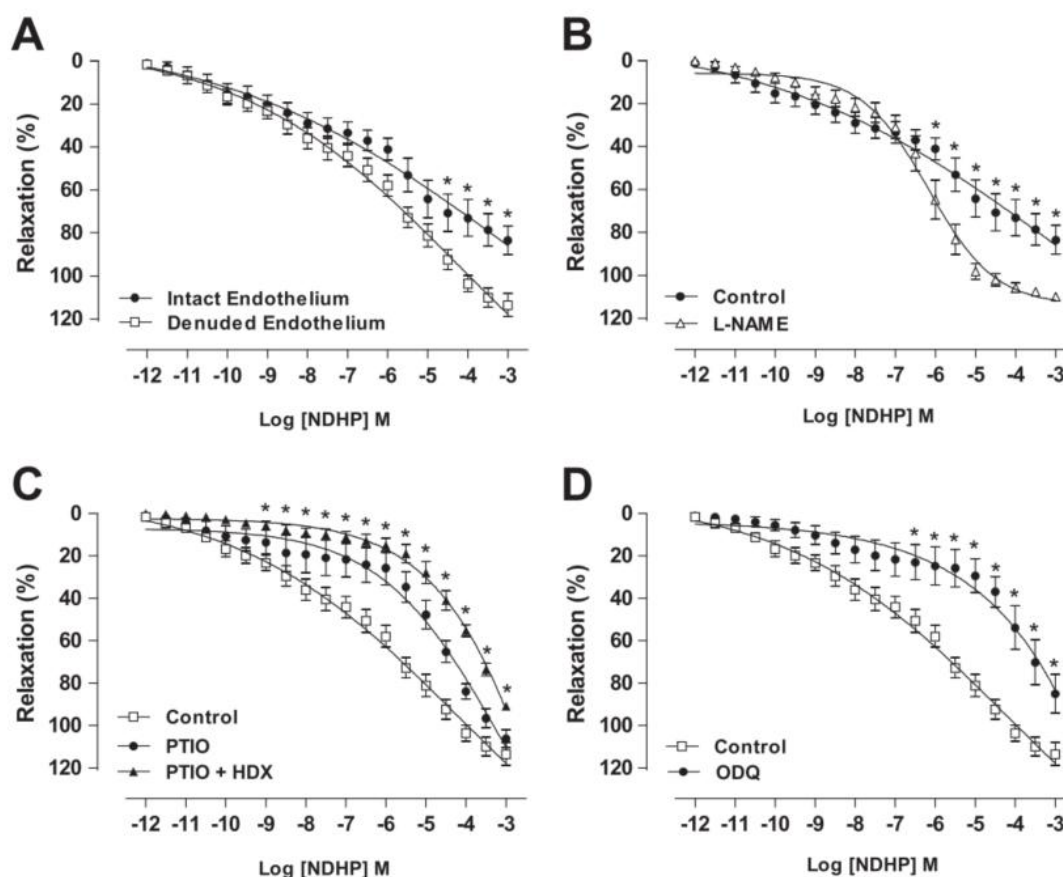

Figure 10. *Role of NO release and signaling in NDHP-mediated vasorelaxation. Concentration-responses induced by NDHP in PHE pre-constricted mesenteric arteries. (A) NDHP induced dose-dependent relaxations in endothelium intact vessels, and denude the endothelium potentiated the relaxations. *p<0.05 versus intact endothelium. (B) NDHP-induced vasorelaxation were increased after inhibition of NOS by L-NAME. *p < 0.05 comparing to intact-endothelium control segments (C, D) Scavenging of NO, using PTIO alone or in combination with HDX, as well as inhibition of sGC with ODQ attenuated NDHP-induced vasorelaxation. *p<0.05 for denuded-endothelium treatment groups versus denuded-endothelium control.*

We also evaluated if NDHP signaling was mediated by formation of NO using 1) the NO scavenger 2-phenyl-4,4,5,5-tetramethylimidazoline-1-oxyl 3-oxide (PTIO) and/or hydroxocobalamin (HDX), and 2) the sGC inhibitor [1,2,4]oxadiazolo[4,3-a]quinoxalin-1-one (ODQ). Following pre-incubation with PTIO, the NDHP response was significantly shifted to the right (i.e. decreased NDHP potency compared to the control; pD2 = 5.1 ± 0.1 vs. 6.5 ± 0.1, p <

0.05) (**Figure 10C**). Moreover, when vessels were pre-incubated with PTIO together with HDX, the right shift of the concentration-response curve was also increased but with a reduction of maximum relaxation (90.8 ± 0.8 vs. control 113.4 ± 5.3%, p<0.05) (**Figure 10C**). Similarly, the sGC inhibitor ODQ decreased NDHP-mediated vasorelaxation compared to the control (Emax = 84.9 ± 9.5 vs control Emax = 113.4 ± 5.3%, p<0.05) (**Figure 10D**). Taken together, the data suggest that NDHP-induced vasodilation can be mediated by NO release and activation of sGC-cGMP pathway.

4.1.6 No indications of NDHP-mediated tolerance in small mesenteric arteries

As already discussed, development of tolerance is a major problem associated with repeated use of organic nitrates [87, 88]. Using mesenteric arteries, we investigated if NDHP treatment was also inducing tolerance. GTN, which was used as a positive control, induced concentration-dependent vasorelaxation, and pre-incubation of vessels with GTN (100 μM) for 30 min induced a clear shift to the right, demonstrating nitrate tolerance (**Figure 11A** and **11B**, pD2 = 7.9 ± 0.10 versus control pD2 = 9.1 ± 0.10, Emax = 100 ± 3% versus control Emax = 124 ± 4%, P < 0.0001).
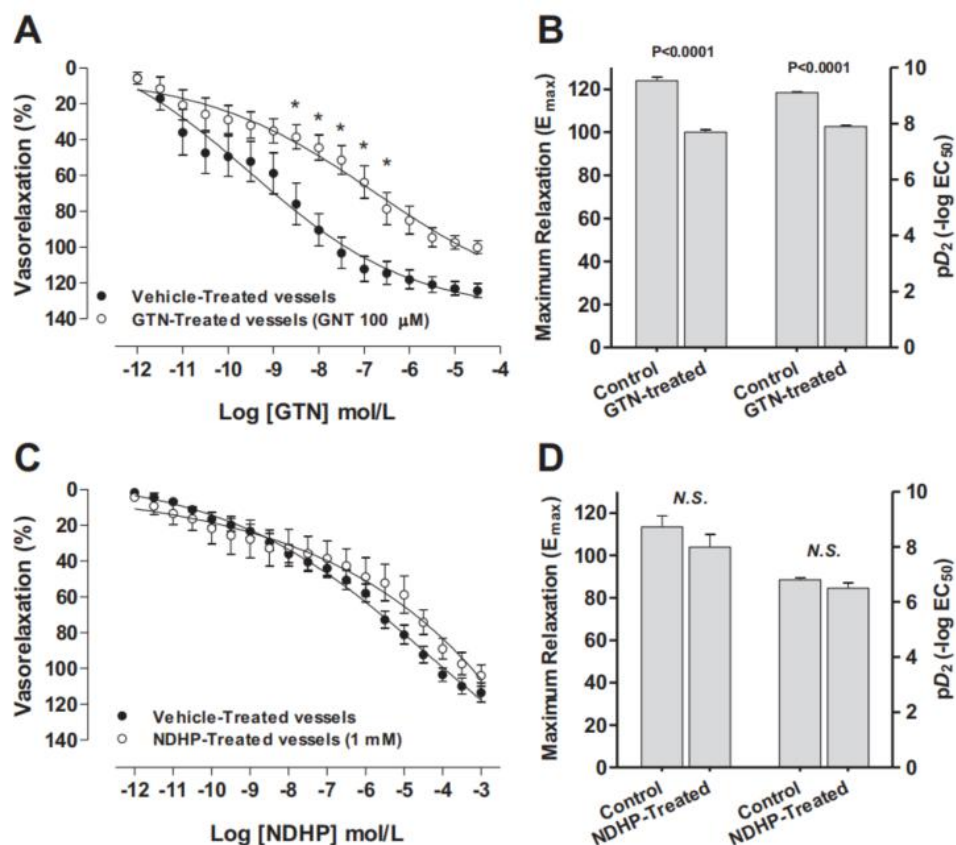

Figure 11. Effects of *NDHP and GTN on tolerance in rat mesenteric arteries. Concentration-response curves for GTN (A) and NDHP (C) in endothelium-denuded superior mesenteric arteries from rats. The potency (pD2) and maximum relaxation effects (Emax) of GTN (B) or NDHP (D) concentration-response curves after vessels were pre-treated for 30 min in GTN (100 μM) or NDHP (100 μM), respectively. * p<0.05 versus vehicle-treated vessels. N.S. = non-significant.*

Conversely, NDHP pretreatment did not induce changes on pD2 (**Figure 11D**; pD2 = 6.5 ± 0.20 versus control 6.8 ± 0.08, P > 0.05) or Emax (**Figure 11D**; Emax = 100 ± 3% versus control 124 ± 4%; P > 0.05). Altogether, these data suggest that in contrast to GTN, NDHP does not induce tolerance in mesenteric arteries.

4.1.7 NDHP reduces blood pressure in 2K1C induced hypertension

As expected, 2K1C surgery induced a baseline MAP increase compared with sham-operated normotensive rats (172 ± 10 vs. 117 ± 2 mmHg). After 6 weeks recovery, acute intravenous administration of NDHP (1; 5; 10; 20 mg/kg) in normotensive rats lowered blood pressure (−11 ± 1; −19 ± 2; −28 ± 2; −44 ± 5 mmHg, respectively). Meanwhile, NDHP (1; 5; 10; 20 mg/kg) also reduced blood pressure in 2K1C hypertensive rats (−16 ± 3; −23 ± 4; −50 ± 1; and −71 ± 8 mmHg, respectively). A significant difference between normotensive and hypertensive rats were found in the doses of 10 and 20 mg/kg (**Figure 12**), suggesting either greater formation or greater sensitivity to NDHP-induced NO in the vascular beds of 2K1C compared with sham-operated animals.
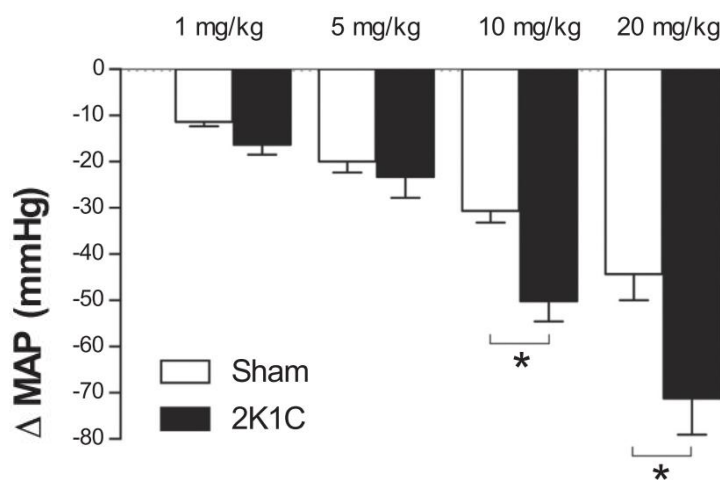

Figure 12. *Changes in mean arterial pressure (ΔMAP) in normotensive and hypertensive-2K1C rats following intravenous administration of NDHP (1, 5, 10 & 20 mg/kg). *p<0.05 between indicated groups.*

4.1.8 NDHP attenuates the progression of L-NAME and Ang II-induced hypertension

Chronic treatment with L-NAME and Ang II significantly increased blood pressure in both vehicle treated group and NDHP treated group, a model of hypertension. However, the blood pressure in NDHP treated group increased less (ΔMAP vehicle: 49mmHg; ΔMAP NDHP: 18mmHg) (**Figure 13A** and **13B**), suggesting treatment with NDHP significantly attenuated the development of hypertension.
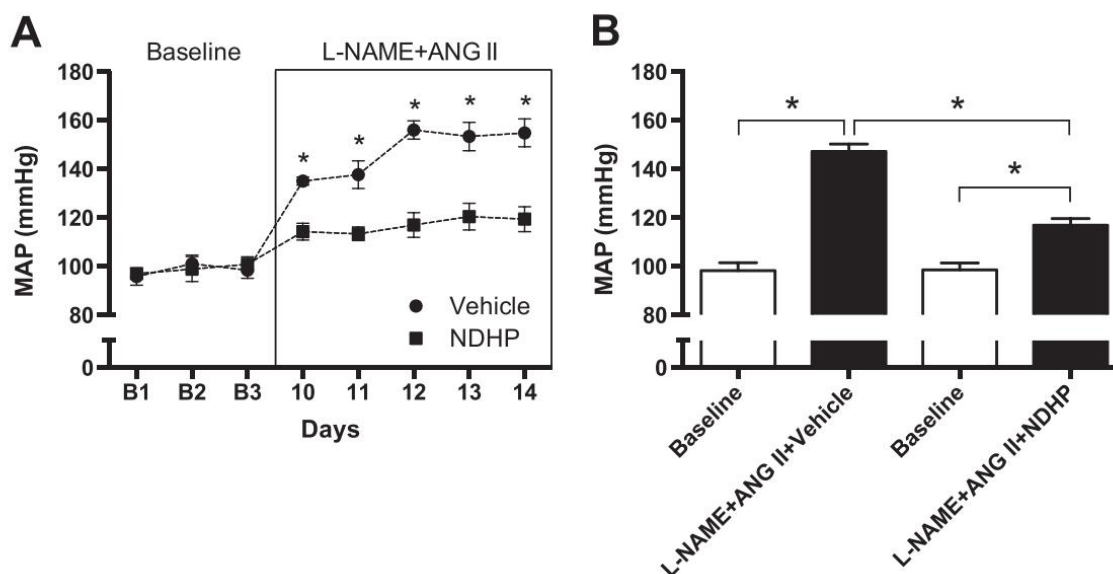
Figure 13. *Effects of chronic treatment with NDHP on blood pressure in an in vivo model of L-NAME and Ang II-induced hypertension. L-NAME (0.5 g/L) was added in drinking water and Ang II was continuously infused subcutaneously (starting at Day 0) using an osmotic pump (infusing Ang II for 14 days). Blood pressure was measured during Baseline (3 days) and during days 10-14 with L-NAME+Ang II treatment. *p<0.05 between the indicated groups.*

4.1.9 Summary – Study I & II

Using a combined experimental approach in Study I and II, with *in vitro*, *ex vivo* and *in vivo* models we show that the newly developed organic mononitrate NDHP is associated with XOR-mediated NO formation and subsequent vasorelaxation of large and small arteries from rats and mice. The effects of NDHP on vessels is independent of functional endothelium and NOS enzyme activity. Moreover, in contrast to that observed with other historically and frequently used organic nitrates, such as GTN, NDHP treatment appears to be void of undesirable tolerance development which is a great advantage. Finally, our findings do not only apply to *in vitro* cell-free systems and *ex vivo* isolated vessel studies but also show promising effects in well characterized *in vivo* hypertension models (*i.e.* 2K1C and chronic Ang II infusion). Although very promising results so far, the therapeutic value of chronic NDHP treatment must be further evaluated in experimental studies before any clinical trials can be discussed/planned.

4.2. Study III: Therapeutic value of inorganic nitrate in renal IR injury

4.2.1 Inorganic nitrate increases markers of NO bioactivity and attenuates renal dysfunction following IR.

Nitrate treatment increased plasma levels of nitrate and nitrite with a trend towards increased plasma cGMP (**Figure 14 A–C**). Renal dysfunction, as reflected by changes in BUN and GFR, were also improved by nitrate (**Figure 14 D- E**).
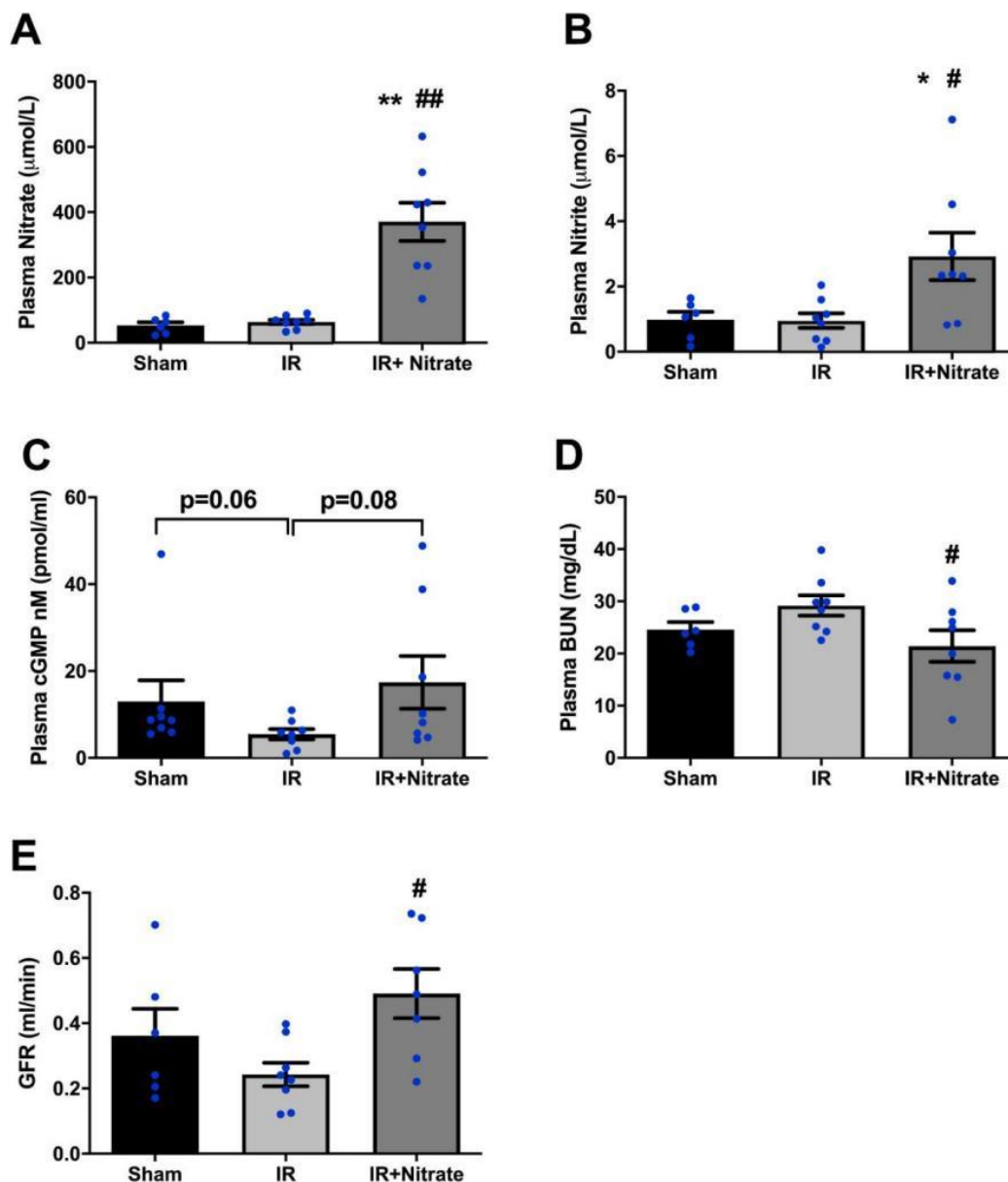

Figure 14. *Effects of nitrate treatment on NO metabolites, cGMP and kidney function following IR of the kidney. Plasma nitrate, nitrite, and cGMP levels (A–C), and BUN and GFR (D–E) following IR in mice treated with placebo or nitrate. *, **p < 0.05 and 0.01 versus Sham group; #, ##p < 0.05 and 0.01 versus IR group.*

4.2.2 Inorganic nitrate attenuates blood pressure responses and renal Ang II levels following IR

Following surgery and two weeks of reperfusion the systolic and mean blood pressure were significantly higher in the IR group compared with sham-operated controls (**Figure 15 A-C**). In IR mice, treated with nitrate, the blood pressure was similar to controls and significantly lower than in IR mice given placebo. To investigate a potential link between elevated blood pressure and changes in RAS, we measured Ang II levels in plasma and in the kidney. We found that Ang II levels in plasma were similar in the three groups, increased in the ischemia kidney compared with controls, but not significantly changed in the contralateral non-ischemia kidney (**Figure 15 D–F**). In agreement with the observed effects of nitrate treatment on blood pressure, the increase of Ang II in the renal tissues following IR was prevented by nitrate. What is the cause and the consequence here is not yet clear, but it is possible that nitrate-nitrite-NO-mediated dampening of RAS activation contributes to the observed antihypertensive effects following IR.
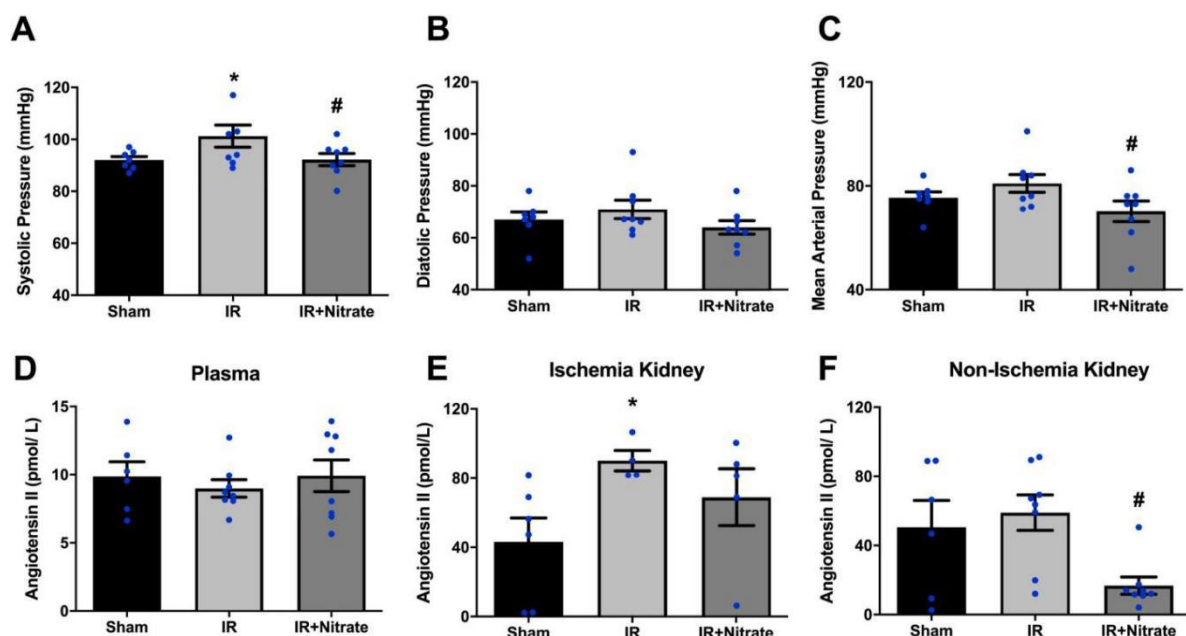

Figure 15. *Systolic, diastolic and mean arterial blood pressure (A-C) and plasma as well as intrarenal levels of Ang II (D-F) following IR in mice treated with placebo or nitrate. *p <0.05 versus sham group, #p < 0.05 versus IR group.*

4.2.3 Inorganic nitrate ameliorates renal histopathological changes, inflammation and apoptosis following IR.

Renal histopathology using H&E and PAS staining was examined after IR. Profound glomerular damage and tubular necrosis was observed in the IR mice compared with sham-operated controls (**Figure 16A-F** and **Table 2**) while nitrate-treated mice displayed less changes, as evident from less cast formation, necrosis, ectasia rupture of tubular basement membrane and more tubular regeneration and necrotic tubules in regeneration (**Figure 16A–F** and **Table 2**). Moreover, F4/80 immunostaining showed substantial infiltration of macrophages in the ischemic kidney following

IR, which was prevented by nitrate treatment (**Figure 17A-B**). TUNEL staining, to detect apoptosis, was significantly elevated after IR injury, which again was significantly reduced by nitrate (**Figure 17C-D**).
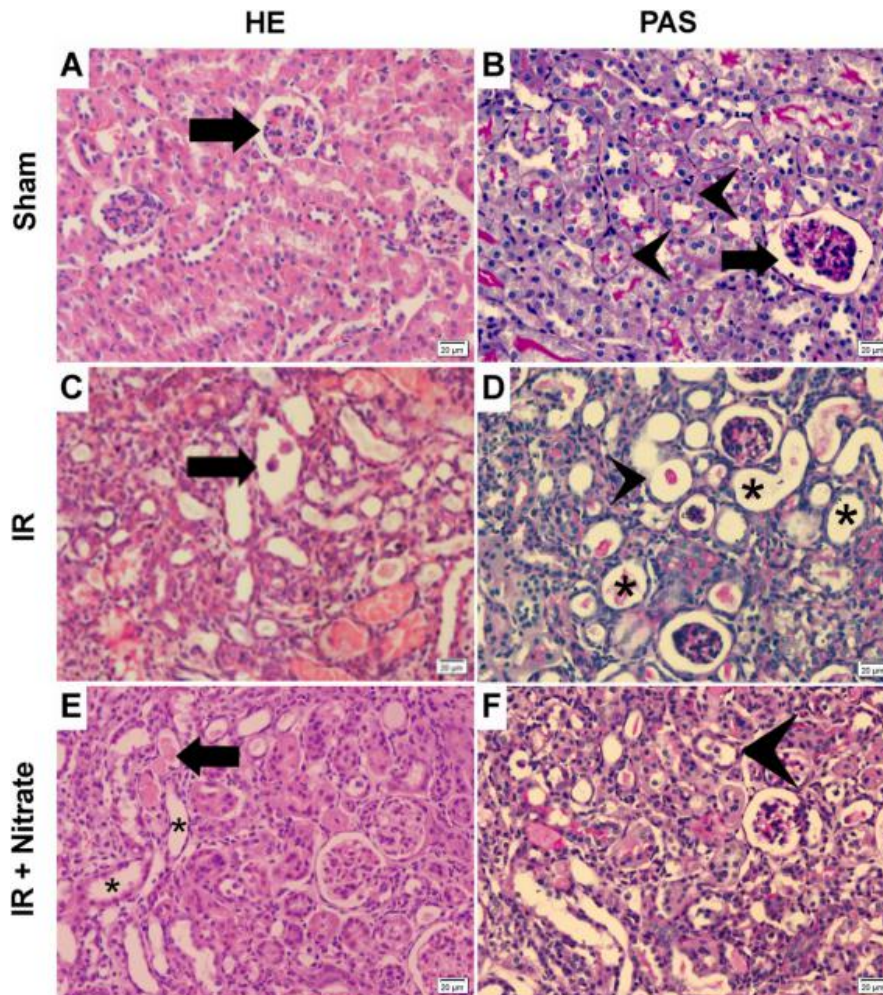

Figure 16. *Effects of nitrate on renal cortex histopathology following IR. Normal renal parenchyma, without glomerular changes, preserved urinary space (arrow), tubules without atrophy or dilation, absence of necrosis and inflammatory cells, and preserved tubular basement membrane (arrowhead) (A–B). Left renal parenchyma submitted to IR showing loss of organ architecture, tubular ectasia (*), tubules with cells in necrosis and lumen filled of cellular debris (arrow), rupture of the tubular basement membrane (arrowhead) and interstitial inflammatory cells (C–D). Left renal parenchyma submitted to IR and treatment with nitrate, presenting necrosis and tubular ectasia (*), presence of granular cylinders in the tubular lumen (arrow), regenerating cells and preserved tubular membranes (arrowhead) (E–F). Magnification is ×400.*
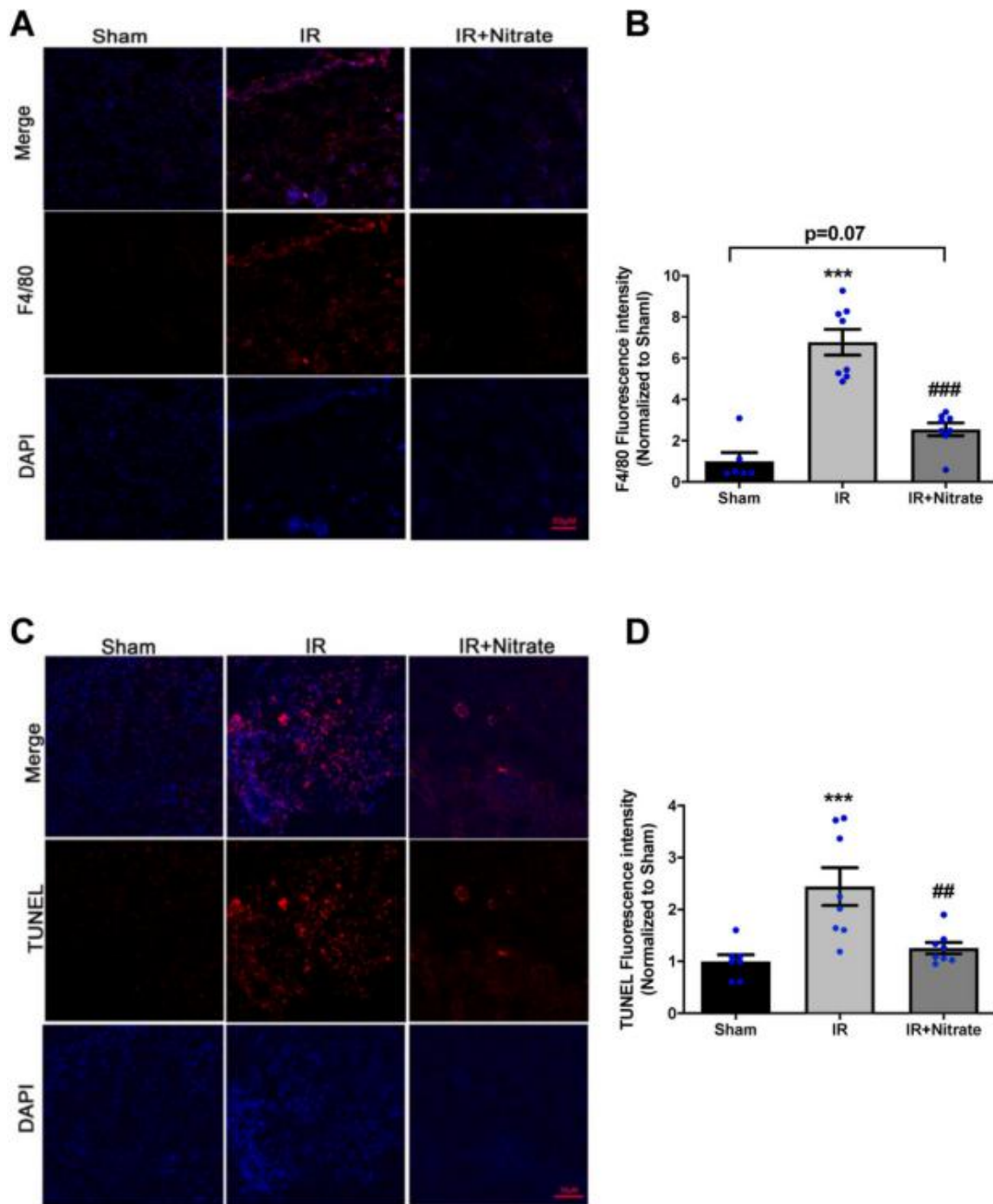
Figure 17. *Effects of nitrate on inflammation and apoptosis following IR of the kidney. Immunostaining images of macrophage infiltration (F4/80, red) in kidneys following IR, counterstained with nuclear marker DAPI. (A) Quantification of F4/80 intensity (B). Immunostaining images of TUNEL (red) (C). Quantification of TUNEL intensity (D). Counterstaining was done using nuclear marker DAPI. Scale bar, 50μm) ***p <0.005 versus sham group, ###p < 0.0001 versus IR group.*

4.2.4 Inorganic nitrate attenuates Ang II-induced contractility of interlobar arteries and afferent arterioles following renal IR

Next, we used the myography technique to assess the effects of IR on vascular function in large intrarenal vessels of the left kidney following reperfusion. Contractility to PHE was not

significantly different between the experimental groups (**Figure 18A**). However, Ang II- induced contractility was significantly increased in the IR kidney (**Figure 18B**), which was prevented by nitrate treatment. In isolated and perfused afferent arterioles (**Figure 18C**), the sensitivity and maximal contractile responses to Ang II were also increased in the IR kidney, which was largely prevented by nitrate treatment (**Figure 18D**).

4.2.5 Inorganic nitrite reduces hypoxia-reoxygenation-induced apoptosis and mitochondrial abnormalities in glomerular endothelial cells

In further vascular mechanistic studies, aimed at mimicking the in vivo IR model, we used GECs. In these cell studies we used nitrite instead of nitrate to bypass the first step in the nitrate-nitrite-NO pathway which requires commensal bacteria in vivo. Hypoxia followed by reoxygenation in GECs reduced cell viability/increased mortality (**Figure 19A-B**). This was associated with increased levels of cleaved caspase-3, reduced mitochondrial complex II and TFAM expression (**Figure 19C–G**), as well as mitochondrial ROS production, as indicated by MitoSox (**Figure 19H**). All these abnormalities associated with hypoxia and reoxygenation were ameliorated by simultaneous treatment with nitrite.

Our *in vivo* and *ex vivo* data indicated that IR-induced injuries and dysfunction were coupled with increased renal Ang II levels (**Figure 15E**) and vascular contractility (**Figure 18B** and **18D**).

Table 2. *Quantification of the histopathological findings (%).*

	Sham	IR	IR + Nitrate
Necrosis	0 ± 0	40.31 ± 3.29 *	23.62 ± 2.43 *, #
Tubular regeneration	0 ± 0	7.80 ± 1.46 *	14.39 ± 2.11 *, #
Necrosis/regeneration ratio	0 ± 0	25.76 ± 7.09 *	60.88 ± 5.33 *, #
Tubular ectasia	0 ± 0	33.87 ± 3.13 *	12.71 ± 1.78 *, #
Rupture of tubular basement membrane	0 ± 0	24.91 ± 2.80 *	8.35 ± 1.07 *, #

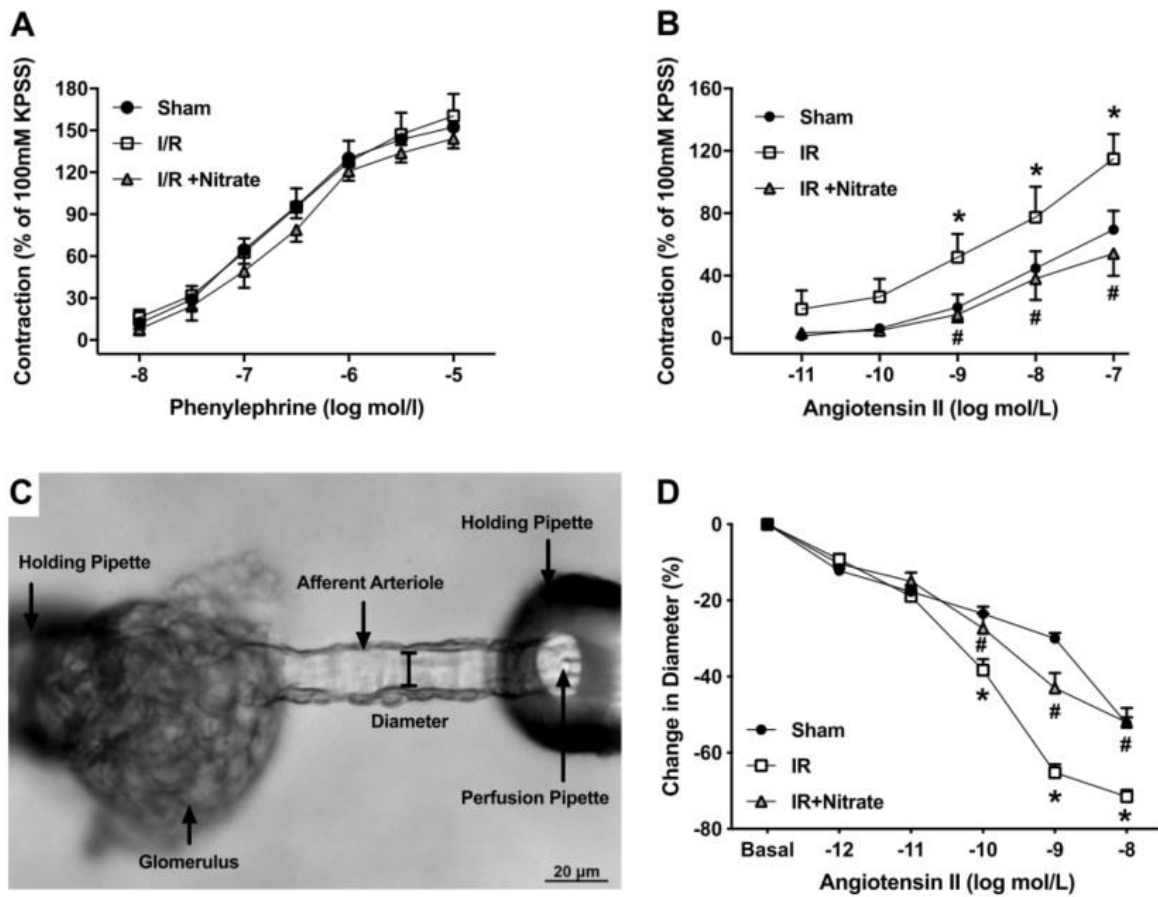*$P<0.05$ versus sham group; #$P<0.05$ versus IR group

Figure 18. *Effects of nitrate treatment on vascular function following IR of the kidney. PHE (A) and Ang II (B) -induced contractions of interlobar arteries. (C) Image of the set-up used for isolated and micro-perfused afferent arterioles. (D) Ang II-induced contractions of arterioles from the ischemic kidney. Changes in luminal diameters are presented as percent of the control diameter. *P<0.05 versus sham group; #P<0.05 versus IR group*
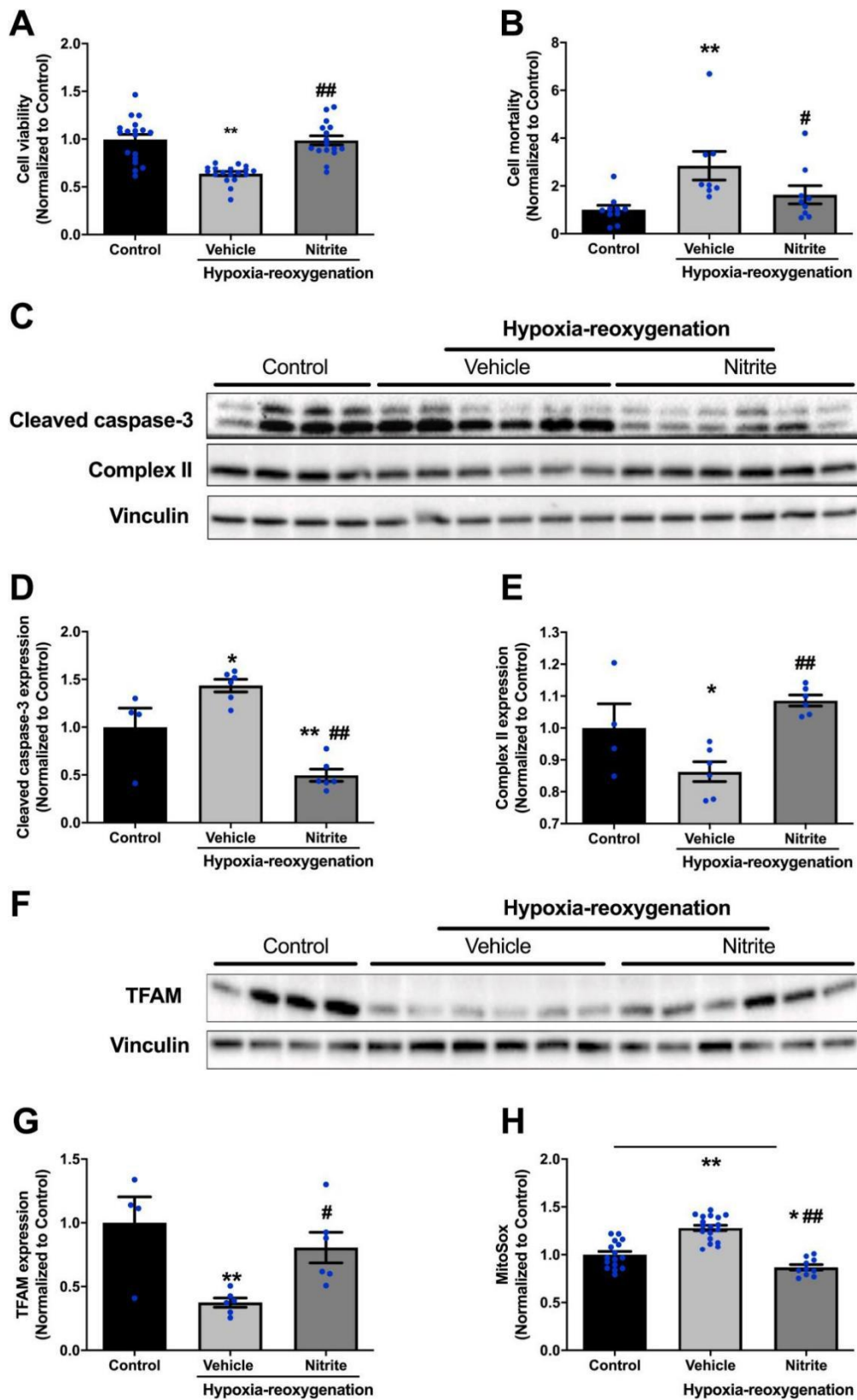
Figure 19. *Effects of nitrite on cell viability/mortality, mitochondrial function/complexes and ROS production following hypoxia-reoxygenation in GEC. Cell viability and mortality (A–B), immunoblotting and quantification of cleaved caspase-3, OXPHOS complex II and (C–E) and TFAM expression (F-G) as well as mitochondrial ROS production as indicated by MitoSox (H) with or without simultaneous nitrite treatment. *, ** p<0.05, 0.01 vs Control; #, ## p<0.05, 0.01 versus vehicle.*

4.2.6 The protective effects of nitrite following hypoxia-reoxygenation in glomerular endothelial cells are abolished by inhibition of XOR

XOR is considered as one of the key enzymes involved in the reduction of nitrite to NO and other bioactive nitrogen oxide species. Here we show that, in the presence of the selective XOR inhibitor febuxostat, the beneficial effects of nitrite on cell viability, TFAM expression and mitochondrial ROS (**Figure 20A–D**) following hypoxia-reoxygenation combined with Ang II in GECs were abolished.
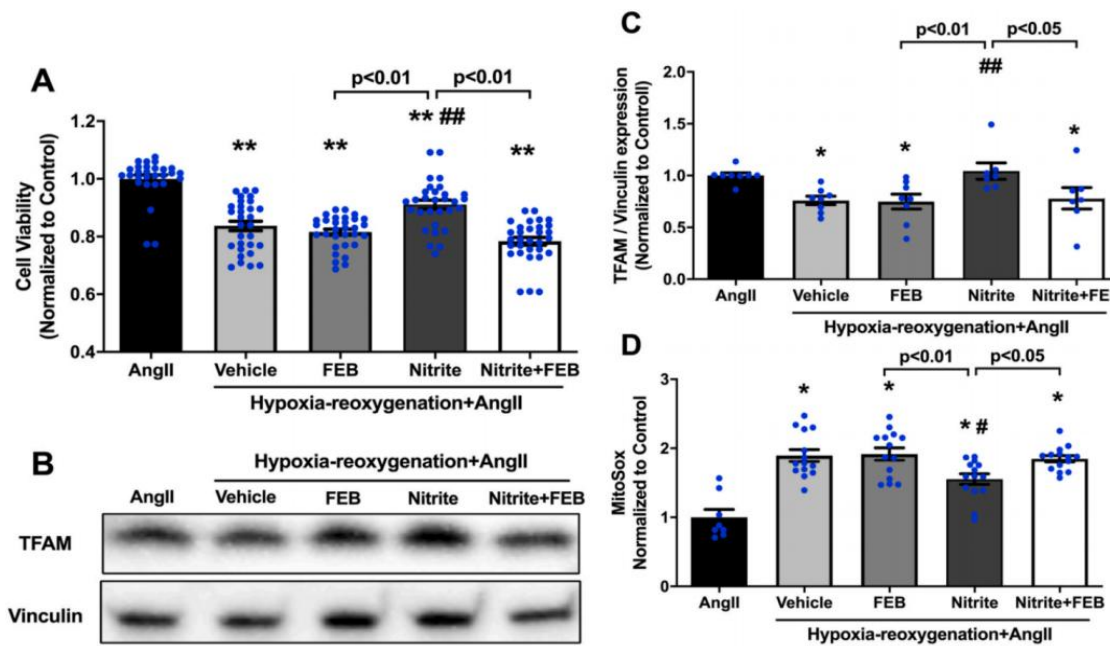

Figure 20. *Effects of nitrite on viability and mitochondrial function in GECs following hypoxia-reoxygenation in combination with Ang II. Nitrite treatment was associated with higher cell viability (A) and TFAM expression (B-C). ROS production, as indicated by MitoSox, was increased following hypoxia-reoxygenation in combination with Ang II (D), which was significantly reduced by nitrite. These favorable effects of nitrite were blocked or at least reduced by pharmacological inhibition of XOR using febuxostat. *, ** p<0.05, 0.01 versus Ang II group; #, ## p<0.05, 0.01 versus vehicle.*

4.2.7 Summary – Study III

Using a combined experimental approach in study III, with *in vitro*, *ex vivo* and *in vivo* models we show that boosting the nitrate-nitrite-NO pathway at the onset of an isolated renal ischemic event and subsequent reperfusion is associated with protective renal and cardiovascular effects. Nitrate/nitrite-mediated formation of bioactive NO species, including NO, was at least in part dependent on functional XOR, which has been reported by us and other groups previously [89-91]. Mechanistically, the favorable effects of nitrate supplementation during the IR period (*in vivo*) and with nitrite treatment in response to hypoxia-reoxygenation of glomerular endothelial cells (*in vitro,* with or without Ang II) dampened kidney injuries, oxidative stress, inflammatory

changes and ameliorated mitochondrial abnormalities. Clinical systematic review and meta-analysis studies have revealed that modifiable life-style factors including dietary habits significantly influence the risks of CVD and kidney disease [14]. In particular, high intake of vegetables was associated with significantly reduced risk of chronic kidney disease [92]. To what extent this can be explained by the high nitrate content in this food group is not yet clear but should be investigated in future clinical studies with dietary nitrate treatment in patients with high risk of AKI and CKD.

4.3 Study IV: Interactions between RBCs and endothelium NOSs

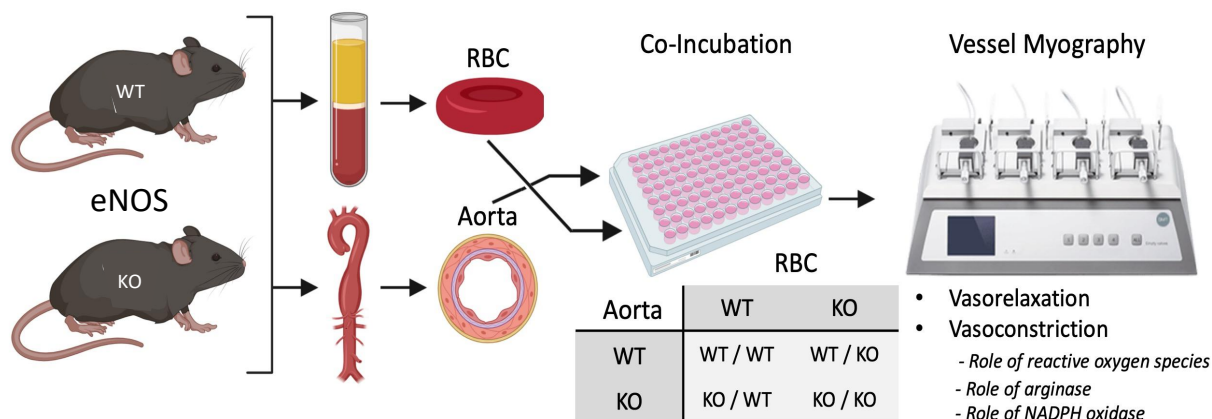The experimental protocol of study IV is highlighted in **Figure 21**.

Figure 21. *Overview of experimental protocol. Aorta and whole blood were isolated from eNOS WT and global eNOS KO mice. Whole blood constituents were separated, and red blood cells (RBC) were washed. Aorta were cleaned and separated into aortic rings in PSS. In indicated combinations, aortic rings and washed RBCs (10% hematocrit, diluted in high glucose; 17.5mM, DMEM) were co-incubated (37 °C; 5% CO2) for 18hrs. Following incubation, aortic rings were washed, and vessel reactivity (vasorelaxation and contractility) was assessed via vascular wire myography. To further assess the role of reactive oxygen species (ROS), arginase and NADPH oxidase (NOX) activity on the observed functional interaction between eNOS KO RBCs and WT aorta, the co-incubations were simultaneously treated with TEMPO (1mM), nor-NOHA (10uM) and selective NOX inhibitor, respectively. In separate experiments, aortic rings and RBCs were collected (after co-incubations) and used for analyses of arginase activity in RBCs.*

4.3.1 RBCs from eNOS KO mice induce endothelial dysfunction

Following overnight (18hr) co-incubation of WT aortas + RBC isolated from eNOS KO mice, a significant reduction in endothelial-dependent relaxation (EDR) was observed, compared with WT vessels co-incubated with WT RBCs (**Figure 22A**). Endothelium independent relaxation was unaffected (EIR; **Figure 22B**).

4.3.2 Abnormal ROS and NO homeostasis contributes to eNOS KO RBC-induced endothelial dysfunction

To investigate whether elevated ROS could play a role, the radical scavenger TEMPOL (1 mM) which has superoxide dismutase and catalase activities was added to overnight co-incubation preparations. TEMPOL significantly preserved the EDR of WT aorta, co-incubated with eNOS KO RBCs, with responses comparable to control vessel vasorelaxations (**Figure 23A**). In all groups, EIR was comparable, and without any effect of TEMPOL (**Figure 23B**).
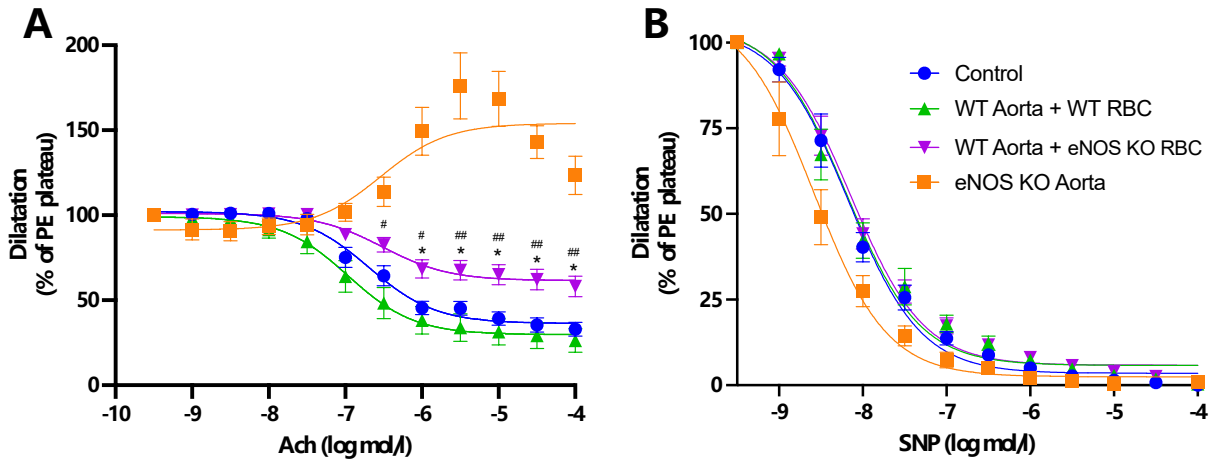
Figure 22. *RBCs from eNOS KO mice induce endothelial dysfunction. (A) Endothelial-dependent vasorelaxation (% of PHE plateau) response curve to Ach (log mol/L) and (B) endothelial-independent vasorelaxation (% of PHE plateau) response curve to sodium nitroprusside (SNP) of mouse aortic rings following overnight (~18hrs) incubation with Control, RBC from a WT mouse (WT RBC; 10%) or RBC from an eNOS KO mouse (KO RBC; 10%). *p<0.05 comparisons of WT aorta + eNOS KO RBC versus control; # p<0.05, ## p<0.01 comparisons of WT aorta + eNOS KO RBC versus WT aorta + WT RBC.*
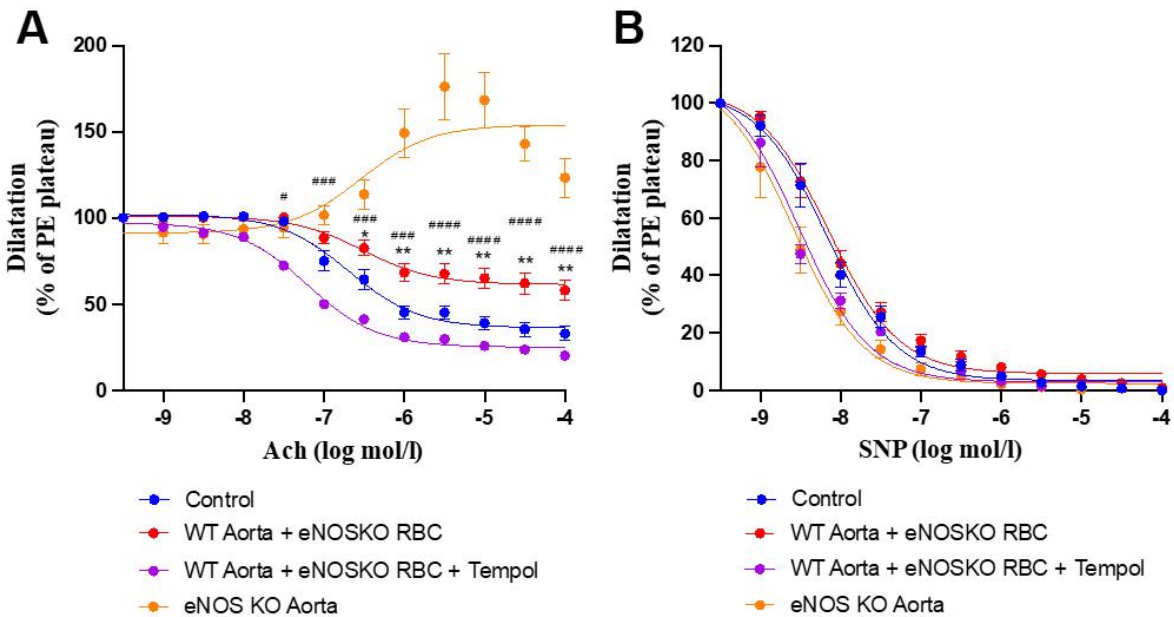

Figure 23. *Functional role of elevated ROS in eNOS KO RBC-induced endothelial dysfunction. (A) Endothelial-dependent vasorelaxation (% of PHE) response curve to Ach (log mol/L), (B) endothelial-independent vasorelaxation (% of PHE) response curve to SNP of WT mouse aortic rings following overnight (~18hrs) incubation with Control, RBC from an eNOS KO mouse (eNOS KO RBC; 10%), +/- TEMPOL (1mM). *p<0.05, **p<0.01, comparisons of WT aorta + eNOS KO RBC versus control; #p<0.05, ###p<0.005, ####p<0.001 comparisons of WT aorta + eNOS KO RBC versus WT aorta + eNOS KO RBC + TEMPOL.*

To further investigate how ROS contributed to the observed eNOS KO RBC-induced endothelial dysfunction, TEMPOL (300uM) was added acutely to the myograph chambers of co-incubated preparations. Similarly, acute tempol significantly preserved EDR following overnight exposure to eNOS KO RBCs (**Figure 24A**). Acute tempol had no effect on aortic ring vasoreactivity following overnight exposure to WT RBCs (**Figure 24C**). Both WT and eNOS KO RBCs EIR responses were comparable to controls following acute incubation with Tempol (**Figure 24B** and **D**).
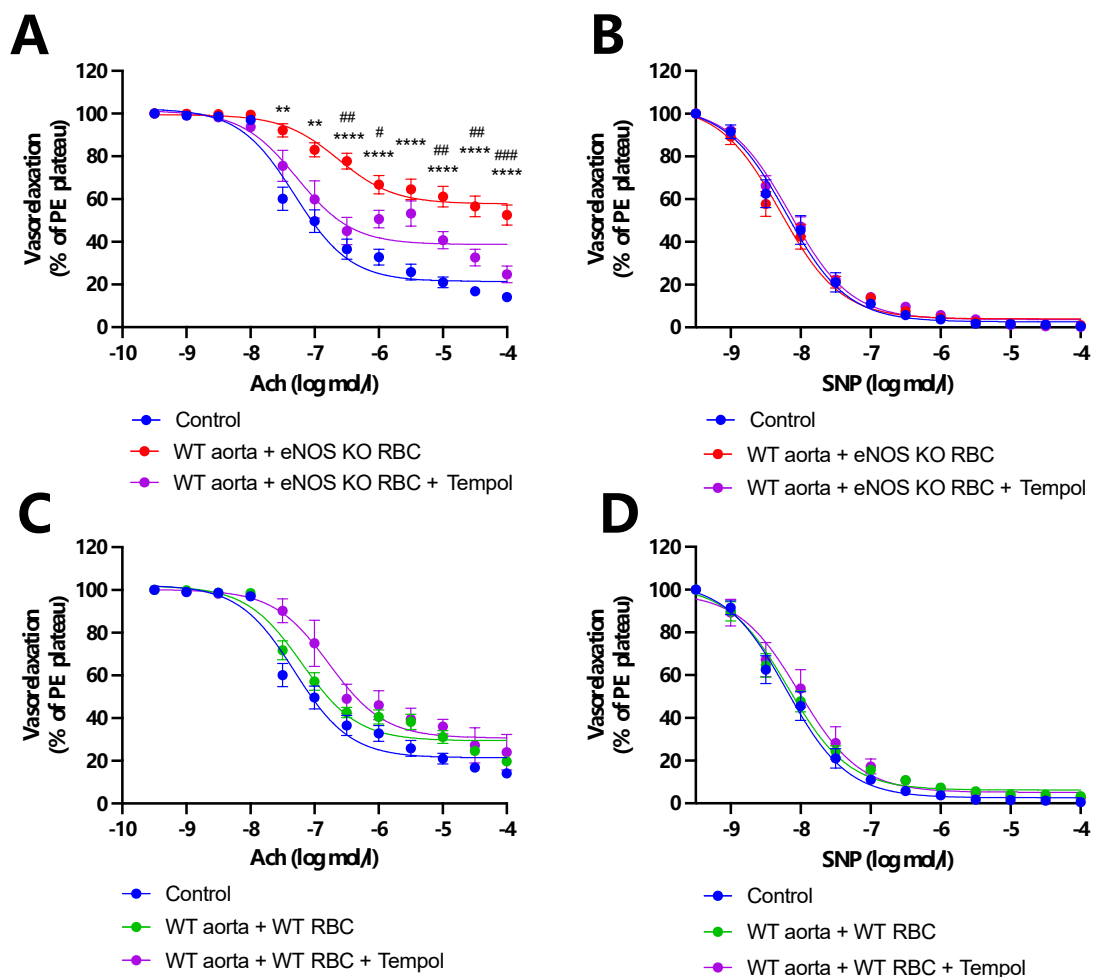

Figure 24. *Functional role of vascular ROS in eNOS KO RBC-induced endothelial dysfunction. (A, C) Endothelial-dependent vasorelaxation (% PHE) response curve to Ach (log mol/L) and (B, D) endothelial-independent vasorelaxation (% PHE) response curve to SNP of WT mouse aortic rings following overnight incubation with Control, (A, B) RBC from an eNOS KO mouse (eNOS KO RBC; 10%), (C, D) RBC from a WT mouse (WT RBC; 10%) with TEMPOL (300uM) added acutely into myograph chamber. **p<0.01; ****p<0.001, comparisons of WT aorta + eNOS KO RBC versus control; #p<0.05, ##p<0.01, ####p<0.001 comparisons of WT aorta + eNOS KO RBC versus WT aorta + eNOS KO RBC + acute TEMPOL.*

In accordance with these findings, incubation of aortic rings following co-incubation with DHE, an index of superoxide (O_2^-) generation, demonstrated significantly increased fluorescent signal

in aortic rings which had been co-incubated with eNOS KO RBCs in comparison with those incubated with WT RBCs (**Figure 25A-B**).

These data suggest an induction of oxidative stress within the endothelium as a result of exposure to RBCs lacking eNOS, and that this increase in ROS generation is maintained following removal of the eNOS KO RBCs.
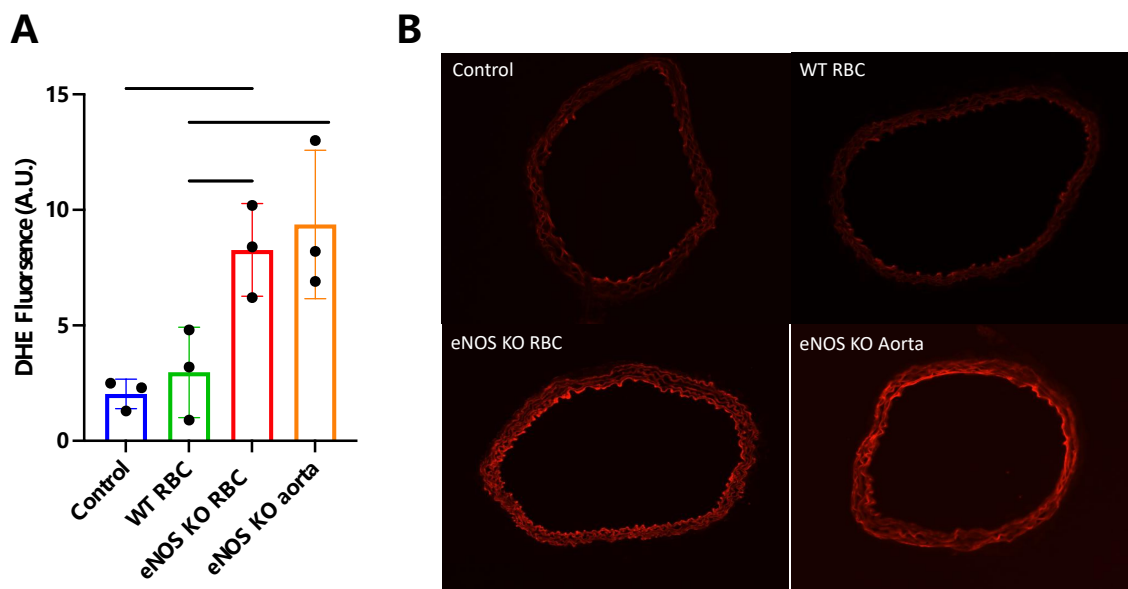

Figure 25. *eNOS KO RBC induce elevated vascular superoxide production measured by DHE fluorescence. (A) Fluorescence intensity of WT mouse aortic rings following overnight (~18hrs) incubation with RBC from an eNOS KO mouse or RBC from a WT mouse. Fluorescence quantified by optic densitometry (arbitrary units). (B) Representative images (x10 magnification) of aortic ring sections incubated in the presence DHE. Red fluorescence produced when DHE is oxidized to 2-hydroxyethidium by $O_2^{\bullet-}$. *p<0.05; **p<0.01 between indicated groups.*

4.3.3 Role of NADPH oxidase in eNOS KO RBC-induced endothelial dysfunction

To determine whether NADPH oxidases (NOXs) were the source of the ROS influencing EDR in this model, we utilized specific pharmacological inhibitors of NOX; a NOX2&4 inhibitor (3 μm) and a NOX4 inhibitor (30 μm) to overnight co-incubation preparations, in separate experiments (**Figure 26**). Simultaneous inhibition of NOX2&4, and sole inhibition of NOX4 both resulted in amelioration of the eNOS KO RBC-induced endothelial dysfunction (**Figure 26A** & **26E**, respectively). NOX inhibition did not alter EIR responses, remaining comparable to controls (**Figure 26B** & **26F**). These data suggest that NOX 2 and 4 contribute to the elevated ROS associated with the detrimental crosstalk between eNOS KO RBCs and the endothelium.
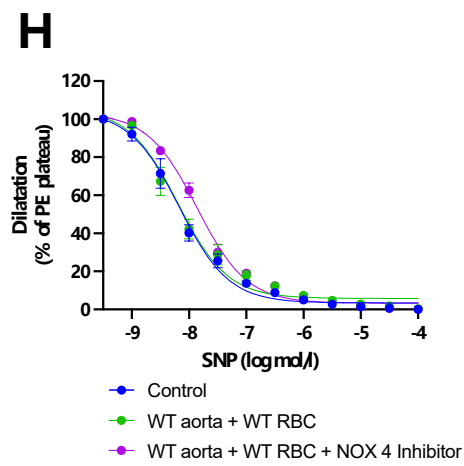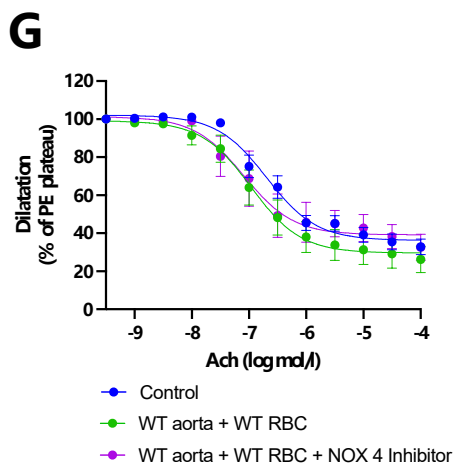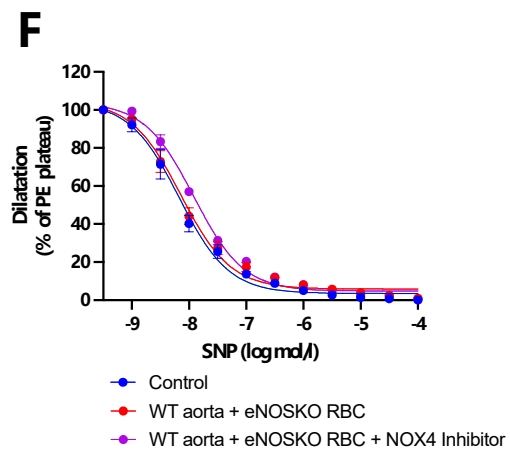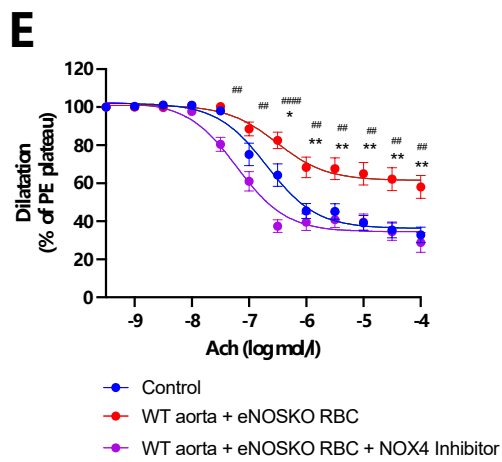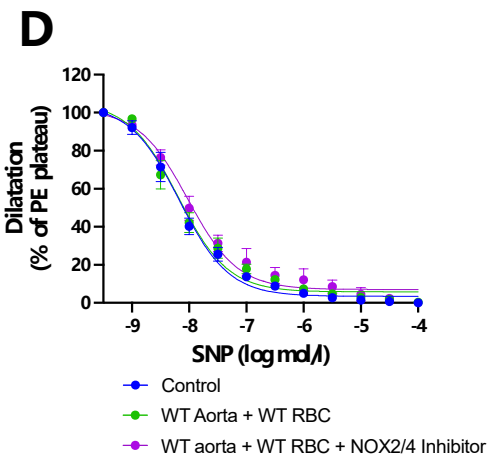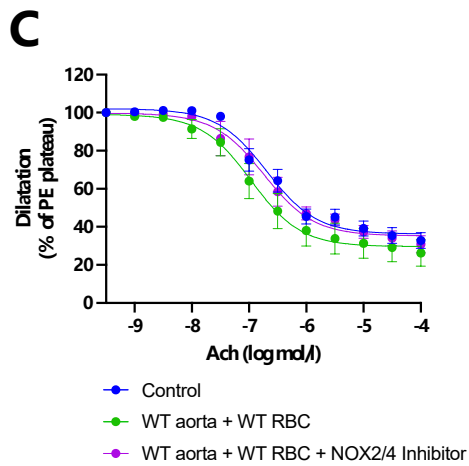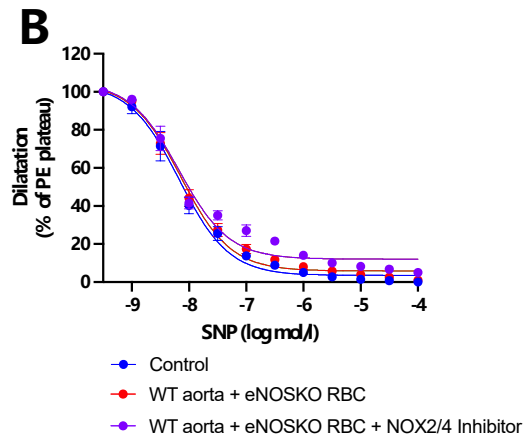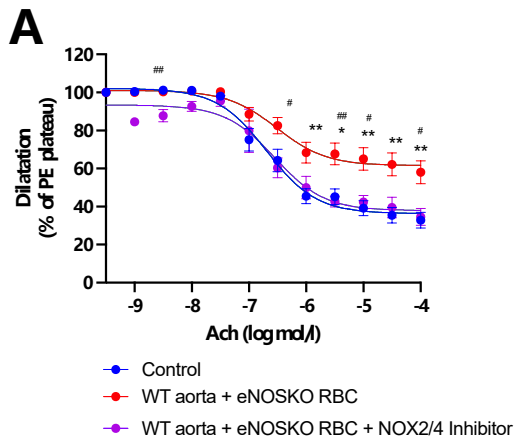
Figure 26. *Functional role of dysregulated elevated ROS in eNOS KO RBC-induced endothelial dysfunction. (A, C, E, G) Endothelial-dependent vasorelaxation (% of PHE) response curve to Ach (log mol/L) and (B, D, F, H) endothelial-independent vasorelaxation (% of PHE) response curve to SNP (log mol/L) of WT mouse aortic rings following overnight (~18hrs) incubation with (A, B) Control, RBC from an eNOS KO mouse (KO RBC; 10%) +/- NOX2&4 inhibitor (3 μM), (C,D) Control, RBC from an WT mouse (WT RBC; 10%) +/- NOX2&4 inhibitor (3 μM). (E, F) Control, RBC from an eNOS KO mouse (eNOS KO RBC; 10%) +/- NOX 4 inhibitor (30 μM). (G, H) Control, RBC from an WT mouse (WT RBC; 10%) +/- NOX 4 inhibitor (30 μM). *p<0.05, **p<0.01, comparisons of WT aorta + eNOS KO RBC versus control; #p<0.05, ##p<0.01, ####p<0.001 comparisons of WT aorta + eNOS KO RBC versus treatments.*

4.3.4 Role of vascular arginase in eNOS KO RBC-induced endothelial dysfunction

In both endothelial cells and RBCs, Arginase 1 competes with eNOS for the common substrate; L-arginine. The balance between the activity of these enzymes is crucial in maintaining eNOS-derived NO bioavailability and cellular redox regulation. We aimed to investigate the influence of arginase in the observed eNOS KO RBC-induced endothelial dysfunction via co-incubating overnight vessel-RBC preparations with the arginase inhibitor nor-NOHA (10 μM). Pharmacological arginase inhibition prevented eNOS KO RBC-induced endothelial dysfunction (**Figure 27A**). EIR was again unaffected (**Figure 27B**). This suggests that RBCs lacking eNOS induce an upregulation of arginase activity, however whether this was predominant in the RBCs *per se,* the endothelium or both was unclear.
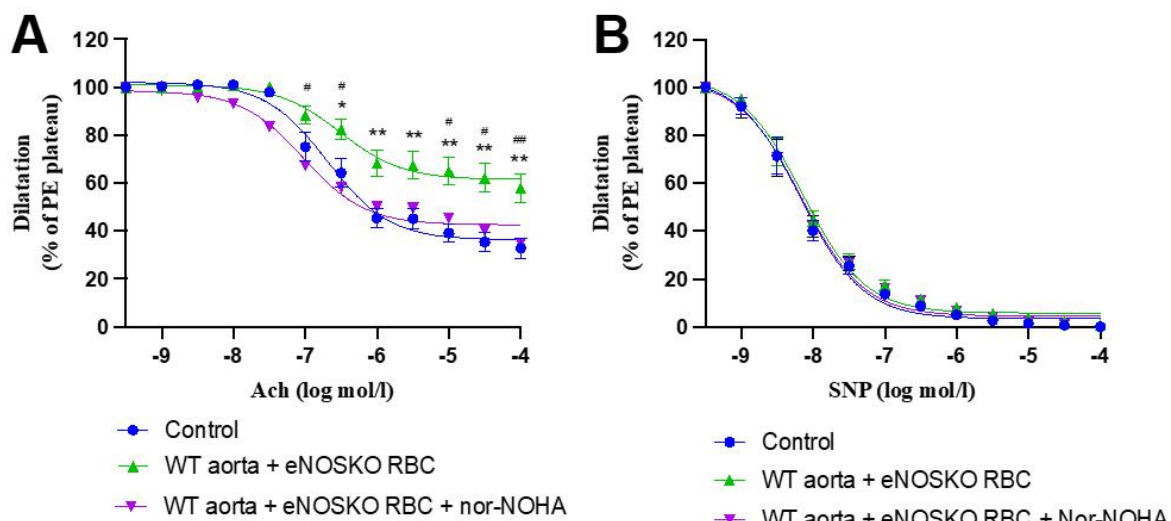
Figure 27. *Functional role of dysregulated Arginase in eNOS KO RBC-induced endothelial dysfunction. (A) Endothelial-dependent vasorelaxation (% of PHE) response curve to Ach (log mol/L) and (B) endothelial-independent vasorelaxation (% of PHE) response curve to SNP (log mol/L) of WT mouse aortic rings following overnight incubation with Control, RBC from an eNOS KO mouse (eNOS KO RBC; 10%) +/- nor-NOHA (10 μM). *p<0.05, **p<0.01; comparisons of WT aorta + eNOS KO RBC versus control; #p<0.05, ##p<0.01, comparisons of WT aorta + eNOS KO RBC versus WT aorta + eNOS KO RBC + nor-NOHA.*

4.3.5 Endothelium-specific Arginase 1 KO vessels are protected from eNOS KO RBC-induced endothelial dysfunction

To address whether endothelial Arginase 1 was directly involved, we utilized a genetic approach via co-incubating endothelial-specific Arginase 1 (Arg1) KO aortas + RBC isolated from eNOS KO mice. We observed EDRs comparable to WT vessels co-incubated with WT RBCs (**Figure 28A**). EIR was unaffected (**Figure 28B**). Together, these data suggest that the transduction of the deleterious interaction between eNOS KO RBC and the endothelium requires endothelial Arginase 1.
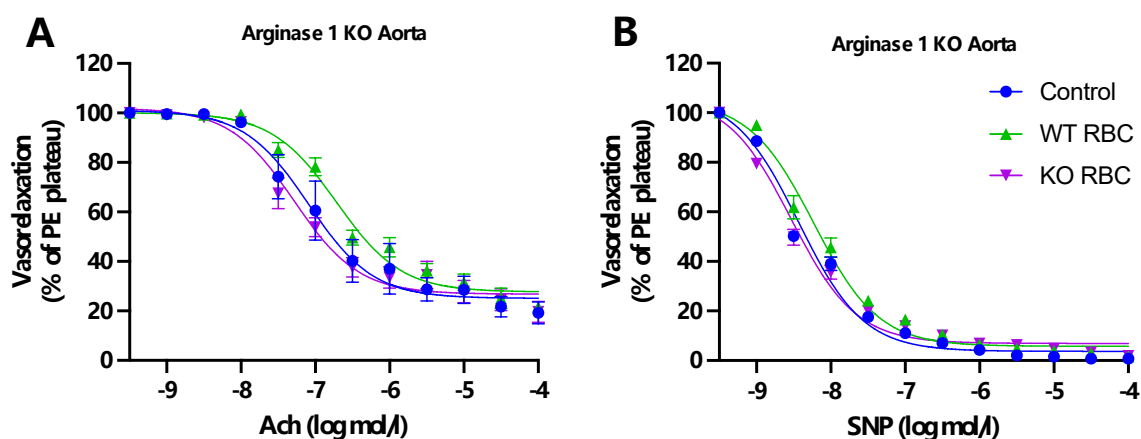
Figure 28. *RBCs from eNOS KO mice do not induce endothelial dysfunction in Arginase 1 KO aorta. (A) Endothelial-dependent vasorelaxation (% of PHE) response curve to Ach (log mol/L) and (B) endothelial-independent vasorelaxation (% of PHE) response curve to SNP (log mol/L) of Arginase 1 KO mouse aortic rings following overnight (~18hrs) incubation with Control, RBC from a WT mouse (WT RBC; 10%) or RBC from an eNOS KO mouse (KO RBC; 10%).*

4.3.6 Arginase activity in RBCs from eNOS KO and WT mice

Next, we aimed to investigate whether RBC arginase may also contribute to the deleterious crosstalk between eNOS KO RBCs and the endothelium. We assessed whether eNOS KO in RBCs results in elevation of RBC arginase activity via quantifying Arginase activity in the membrane fractions of RBCs from eNOS KO vs WT mice. No significant differences were observed (**Figure 29**). This suggests that within the RBC membrane, a lack of eNOS *per se*, does not influence arginase activity. Further, that the role of Arginase 1 in the mediation of the deleterious crosstalk between eNOS KO RBC and endothelium is solely localized to the endothelium.
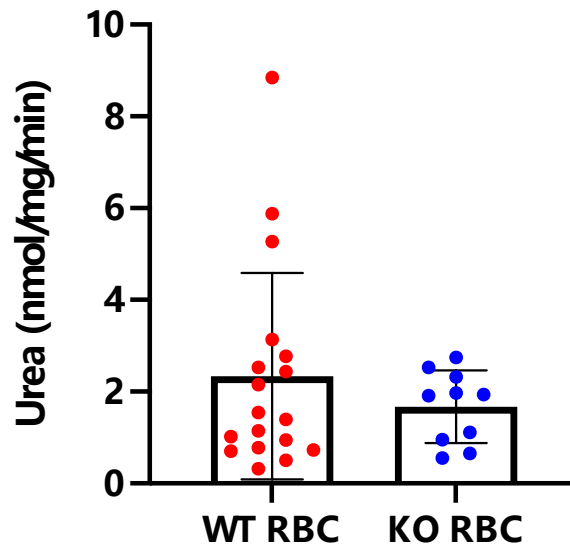
Figure 29. *Arginase activity in membrane fractions of RBCs from eNOS KO and WT mice.*

4.3.7 Effect of supernatant-derived factor(s) on vascular function

To further assess the eNOS KO RBC-endothelial interaction, we incubated washed RBCs (WT and eNOS KO) with DMEM media (Glucose 17.5mM) for 18hrs, and subsequently collected the supernatant for co-incubation (18hrs) with WT aorta for vascular reactivity analyses. However, no differences in PHE-induced contractility, EDR or EIR were observed between Control, WT RBC and eNOS KO supernatants (**Figure 30 A-C**).
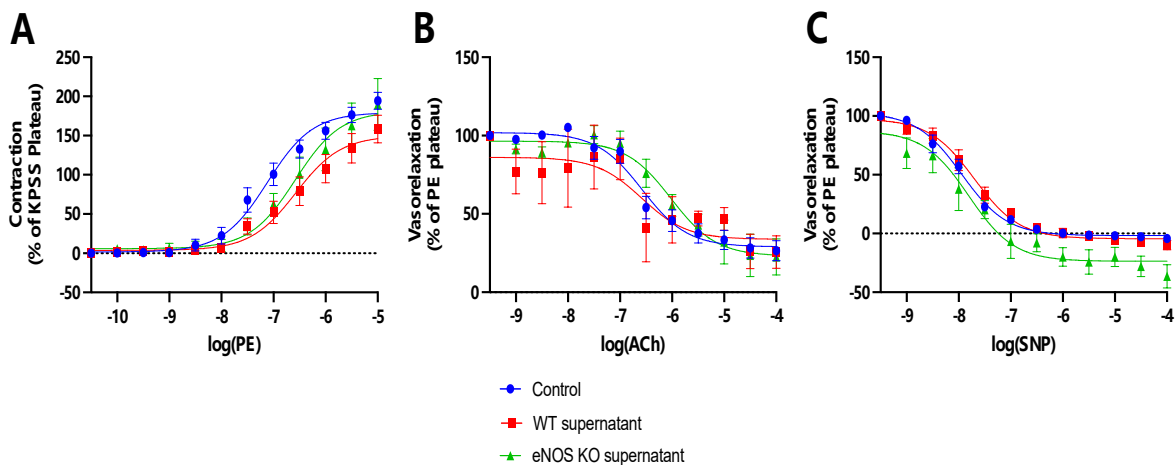
Figure 30. *Supernatant, collected following 18hr co-incubation with eNOS KO RBCs, does not induce endothelial dysfunction. (A) Vasocontractile response curve (% KPSS plateau) to PHE, (B) endothelial-dependent vasorelaxation in response to ACh and (C) endothelial-independent vasorelaxation in response to SNP of WT mouse aortic rings following overnight (~18hrs) incubation with supernatant's collected following 18hr incubation with Control, RBC from a WT mouse (WT RBC; 10%) or RBC from an eNOS KO mouse (KO RBC; 10%).*

4.3.8 Role of hemolysis in eNOS KO RBC-induced endothelial dysfunction

We next aimed to examine whether the release of a factor via hemolysis accounted for the observed eNOS KO RBC-induced endothelial dysfunction. Lysed WT (**Figure 31A**) and eNOS RBCs (**Figure 31B**), with a known % hemolysis, were co-incubated (18hrs) with WT aortic rings and subsequently vascular reactivity was assessed. Marked endothelial dysfunction was only observed in aortic rings incubated with 1.5% hemolyzed RBCs. No differences between maximal ACh-induced vasorelaxation was observed between lysed WT and eNOS KO RBCs at each % lysis (**Figure 31C**).
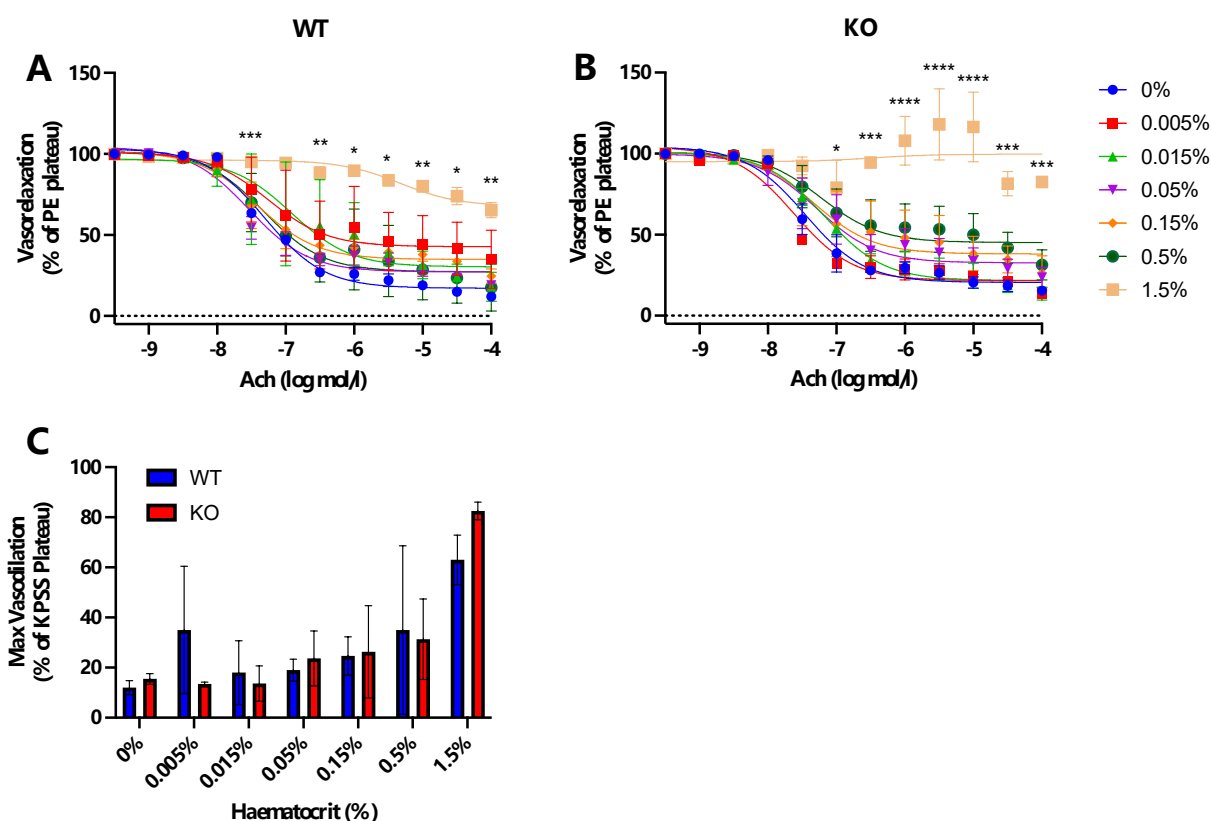
Figure 31. *Only Lysed RBCs above 1.5% hematocrit induce endothelial dysfunction following overnight incubation. Endothelial-dependent vasorelaxation in response to ACh of WT aortic rings following overnight (18hr) co-incubation with lysed (A) WT and (B) eNOS KO RBCs, at increasing concentrations. (C) Max vasodilation (ACh 100 μM) following ACh dose-response. 0% hematocrit denotes incubation with DMEM media without RBC. % denotes % lysed RBCs in DMEM media. *p<0.05, **p<0.01, ***p<0.001, ****p<0.0001 vs 0% lysed RBCs.*

In the same preparations, following co-incubation (18hrs), supernatants were collected, and hemoglobin was quantified (**Figure 32**). No significant difference in hemolysis (%) was observed between supernatants collected post co-incubation with WT vs eNOS KO RBCs (0.032 ± 0.005 vs $0.033\pm0.004\%$, respectively).
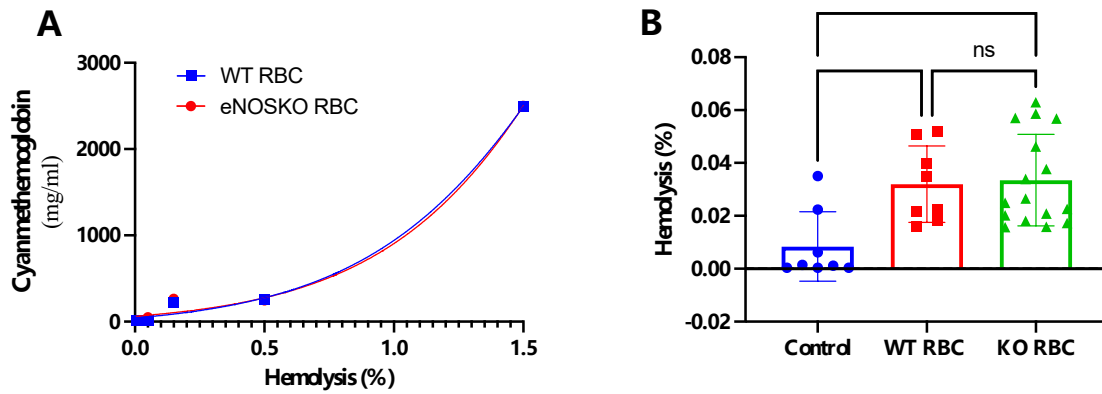
Figure 32. *No difference in hemolysis measurements (%) between supernatants of following 18hr co-incubation of WT vs eNOS KO RBCs and WT aortas. (A) Standard curve of known hemolysis concentrations (%) and corresponding cyanmethemoglobin concentrations (mg/ml) as measured via the Drapkin method. (B) Interpolated cyanmethemoglobin concentration values of supernatant samples collected post 18hr co-incubation of WT vs eNOS KO RBC + WT aorta preparations. Control denotes supernatants collected following overnight incubation of WT aorta with DMEM media without RBC. *p<0.05; **p<0.01.*

4.3.9 Summary – Study IV

Using a combined experimental approach in Study IV, with *in vitro* and *ex vivo* models, we show the existence of communication/interaction between RBCs and adjacent endothelium in regulation of vascular function. The potential role of eNOS RBCs-mediated export of NO bioactivity has been greatly debated for several years. From our findings it is clear that RBCs lacking eNOS can induce significant endothelium dysfunction, which appears to be coupled with endothelial Arg-1 activity, oxidative stress and reduced NO bioavailability. Similar findings of RBC-induced endothelium dysfunction have been demonstrated in patients with type 2 diabetes and in women with pre-eclampsia [76, 79]. Apart from the possibility of disturbed NO export/homeostasis, the signaling molecule(s) contributing to this detrimental interaction between RBCs and the vasculature is not yet fully known, but does not seem to linked with increased hemolysis or release of free heme.

5 CONCLUSIONS

- **STUDY I**: Synthesis and characterization of a novel organic mononitrate NDHP are described. Following treatment with NDHP, this organic nitrate can be reduced to NO by XOR and induce vasorelaxation of mesenteric arteries of rats and mice. *In vitro* findings suggest that NDHP does not induce tolerance, as is the case with GTN, and may therefore serve as a good candidate for future clinical use.

- **STUDY II**: Acute treatment with NDHP increases NO formation, which is associated with vasorelaxation and a significant reduction of blood pressure in hypertensive animals. Chronic NDHP treatment attenuates the progression of hypertension and endothelial dysfunction, suggesting a potential for therapeutic applications in CVD.

- **STUDY III**: Treatment with inorganic nitrate, which is found in high levels in certain foods, may serve as a novel therapeutic approach to prevent development of AKI and CKD, and associated risk of cardiovascular dysfunction, following renal IR.

- **STUDY IV**: RBC eNOS has a regulatory role on vascular endothelial function, which at least in part involves modulation of arginase and NADPH oxidase function/activity. This provides novel insights into the functional relationship between RBCs and adjacent vessels during health and CVD.

6 FUTURE PERSPECTIVES

- The most undesired side-effect of current clinical used organic nitrates is so-called nitrate tolerance. In this regard, the development of novel organic nitrates with similar/higher potency and fewer side effects has attracted the attention of many scientists. In study I and II, a new organic mononitrate, NDHP, was synthesized and its cardiovascular properties were functionally characterized. NDHP induced significant vasorelaxation effects *ex vivo* and reduction of blood pressure *in vivo* through the enzyme XOR. Importantly, in contrast to GTN, repeated applications of NDHP even in high doses did not induce nitrate tolerance, which indicated potential future therapeutic value.

- In clinical practice, it is very important to identify risks and find effective methods/strategies to prevent the development of acute kidney injury, especially when patients undergo an elective surgery. In study III, we found that treatment with a bolus dose of inorganic nitrate 2 hours prior to AKI surgery and followed by daily dietary supplementation of nitrate significantly attenuated kidney damages and associated pathologies. This new treatment strategy may have potential therapeutic value in the future.

- The discovery of functional NOS in RBCs has provoked a great deal of debate regarding its potential ability to interact with NOS in the endothelium and thereby affect vascular function. In study IV, we provided solid evidence that RBCs from mice lacking eNOS can induce endothelium dysfunction in otherwise healthy control vessels. Mechanistically, this pathological vascular phenotype, involves interaction and modulation induced by arginase activity and oxidative stress. Our findings do not only provide novel ideas for studying underlying mechanisms involved in the crosstalk between RBCs and the endothelium, but do also emphasize potential new therapeutic strategies for modulation of RBC/endothelium interaction.

7 ACKNOWLEDGEMENTS

My PhD has been an amazing journey not only of scientific work but also fostering of social connections and the development of positive personal behaviours. This PhD would have been impossible without the help of numerous people. In particular, I would like to thank:

Mattias Carlström, my main supervisor. Thank you for accepting me into your research group and for your constant patience and understanding. I learned a lot from you, not only your technical skills *e.g.,* kidney surgery, hypertension models, but also the crucial skills required to excel in research, such as organisation and how to construct a high-quality scientific paper. The period spent working in your group has been one of the most important, formative experiences of my life. Many thanks again.

Eddie Weitzberg, my co-supervisor. You are a kind and knowledgeable person, who offered me a lot of help with project design, experimental procedures, data interpretation and manuscript writing. I am grateful your door was always open for everyone to discuss their projects with you at any time. Your optimism and positive attitude impacted me deeply.

Jon Lundberg. Thank you very much Jon, you offered me huge amounts of help in many ways. I am always inspired by your plentiful knowledge of our research field, you are the wisest man in our lab and have provided me with such valuable guidance. You also taught me (by example) how to answer questions through a scientific lens and how to be a qualified scientist. These experiences will serve me for life.

Marcelo Montenegro, my co-supervisor. It's been a long time since you left our lab, but I still want to express my gratitude to you. Every single day with you was enriching, your ideas were always crazy, but you could always turn out interesting scientific results. Thank you for all your input on my projects, hope we can meet again soon.

EnYin Lai, my co-supervisor and the driving force for my move to Sweden. It was a happy and memorable period when I stayed in your lab before I came to Sweden. I learned many useful techniques from you and from colleagues in your lab.

Eva Lindgren, my mentor. Thank you for your continued concern and support. I feel very lucky that you were my mentor and I am deeply grateful for all your kind help.

Sarah McCann Haworth, my colleague and dear friend. Sarah, thank you very much for all your input in my projects and papers, and for all of the fantastic memories that we have. We do experiments together, discuss results together and also write papers together. More specifically,

the relationship we have is beyond the ordinary colleague, you are even my daughter Cathy's English teacher and she likes you very much.

Annika and Carina, ladies of our lab. Thank you for your kind and selfless help in every aspect of my life in Sweden and for contributing your knowledge and skills to help me with experiments. Thank you for your stories about Swedish culture and history and all the useful tips. It is no exaggeration to say that you are both walking encyclopaedias!

To all the other colleagues in the lab: **Andrei Kleschyov,** we have been working together since 2017, and we will definitely have more research collaborations in the future. **Drielle D Guimarães,** it was nice to work with you and learn about Brazil, alongside **Josiane C Cruz, Luciano L Paulo**. The person with the largest lung capacity in our lab, **Tomas Schiffer,** you were very kind to everyone and thank you for the great input in anything mitochondria-related. **Gensheng Zhang, Huirong Han and Xuechen Li,** although we did not work together for long, we developed a deep friendship. Hope can meet you again in the future. **Miriam M. Cortese-Krott,** a special thank you for the precious knockout mice you generously provided to us.

And also special thanks to **Mikael Adner** from IMM and all his group members, especially **Jesper Säfholm, Maria Belikova, Willem Abma, JieLu Liu, Mu Nie, Caijuan Dong, Lingling Wu**.

Thanks to my family who always supported me unconditionally. 感谢我的女儿诸葛芷玥 Cathy，你是我的天使，也是我完成学业的最大动力。同时感谢我的家人一直以来对我的理解和关心，如果没有你们的全力支持，我甚至都不可能前来瑞典就读博士。谢谢你们的牺牲和付出！

这里给我女儿展示一段祖训。诫子书成书于公元 234 年，家族祖祖辈辈流传至今，是我们中华文化的瑰宝之一。"淡泊明志，宁静致远"，可作为你的人生信条。希望在你漫长的人生中，能够时刻记住我们全家人对你的殷切期盼。

<div align="center">诸葛亮·【诫子书】</div>

　　夫君子之行，静以修身，俭以养德。非淡泊无以明志，非宁静无以致远。夫学须静也，才须学也，非学无以广才，非志无以成学。淫慢则不能励精，险躁则不能治性。年与时驰，意与日去，遂成枯落，多不接世，悲守穷庐，将复何及！

8 REFERENCES

1.   Tomimatsu, T., et al., *Pathophysiology of preeclampsia: an angiogenic imbalance and long-lasting systemic vascular dysfunction.* Hypertens Res, 2017. **40**(4): p. 305-310.

2.   Tuttolomondo, A., M. Daidone, and A. Pinto, *Endothelial Dysfunction and Inflammation in Ischemic Stroke Pathogenesis.* Curr Pharm Des, 2020. **26**(34): p. 4209-4219.

3.   Camici, P.G., et al., *Coronary microvascular dysfunction in hypertrophy and heart failure.* Cardiovasc Res, 2020. **116**(4): p. 806-816.

4.   Marti, C.N., et al., *Endothelial dysfunction, arterial stiffness, and heart failure.* J Am Coll Cardiol, 2012. **60**(16): p. 1455-69.

5.   Panza, J.A., *Endothelial dysfunction in essential hypertension.* Clin Cardiol, 1997. **20**(11 Suppl 2): p. II-26-33.

6.   Polovina, M.M. and T.S. Potpara, *Endothelial dysfunction in metabolic and vascular disorders.* Postgrad Med, 2014. **126**(2): p. 38-53.

7.   Santoro, D., et al., *Endothelial dysfunction in chronic renal failure.* J Ren Nutr, 2010. **20**(5 Suppl): p. S103-8.

8.   Widmer, R.J. and A. Lerman, *Endothelial dysfunction and cardiovascular disease.* Glob Cardiol Sci Pract, 2014. **2014**(3): p. 291-308.

9.   Furchgott, R.F. and J.V. Zawadzki, *The obligatory role of endothelial cells in the relaxation of arterial smooth muscle by acetylcholine.* Nature, 1980. **288**(5789): p. 373-6.

10.   Palmer, R.M., A.G. Ferrige, and S. Moncada, *Nitric oxide release accounts for the biological activity of endothelium-derived relaxing factor.* Nature, 1987. **327**(6122): p. 524-6.

11.   Ignarro, L.J., et al., *Endothelium-derived relaxing factor from pulmonary artery and vein possesses pharmacologic and chemical properties identical to those of nitric oxide radical.* Circ Res, 1987. **61**(6): p. 866-79.

12.   Carlstrom, M., J.O. Lundberg, and E. Weitzberg, *Mechanisms underlying blood pressure reduction by dietary inorganic nitrate.* Acta Physiol (Oxf), 2018. **224**(1): p. e13080.

13.   Farah, C., L.Y.M. Michel, and J.L. Balligand, *Nitric oxide signalling in cardiovascular health and disease.* Nat Rev Cardiol, 2018. **15**(5): p. 292-316.

14.   Carlstrom, M., *Nitric oxide signalling in kidney regulation and cardiometabolic health.* Nat Rev Nephrol, 2021. **17**(9): p. 575-590.

15. Fish, J.E. and P.A. Marsden, *Endothelial nitric oxide synthase: insight into cell-specific gene regulation in the vascular endothelium.* Cell Mol Life Sci, 2006. **63**(2): p. 144-62.

16. Forstermann, U. and W.C. Sessa, *Nitric oxide synthases: regulation and function.* Eur Heart J, 2012. **33**(7): p. 829-37, 837a-837d.

17. Xue, Q., et al., *Regulation of iNOS on Immune Cells and Its Role in Diseases.* Int J Mol Sci, 2018. **19**(12).

18. Ungvari, Z., et al., *Mechanisms of vascular aging: new perspectives.* J Gerontol A Biol Sci Med Sci, 2010. **65**(10): p. 1028-41.

19. Seals, D.R., K.L. Jablonski, and A.J. Donato, *Aging and vascular endothelial function in humans.* Clin Sci (Lond), 2011. **120**(9): p. 357-75.

20. Despres, J.P., *Body fat distribution and risk of cardiovascular disease: an update.* Circulation, 2012. **126**(10): p. 1301-13.

21. Carlstrom, M. and M.F. Montenegro, *Therapeutic value of stimulating the nitrate-nitrite-nitric oxide pathway to attenuate oxidative stress and restore nitric oxide bioavailability in cardiorenal disease.* J Intern Med, 2019. **285**(1): p. 2-18.

22. Tejero, J., S. Shiva, and M.T. Gladwin, *Sources of Vascular Nitric Oxide and Reactive Oxygen Species and Their Regulation.* Physiol Rev, 2019. **99**(1): p. 311-379.

23. Zhang, L., et al., *Biochemical basis and metabolic interplay of redox regulation.* Redox Biol, 2019. **26**: p. 101284.

24. Forstermann, U., N. Xia, and H. Li, *Roles of Vascular Oxidative Stress and Nitric Oxide in the Pathogenesis of Atherosclerosis.* Circ Res, 2017. **120**(4): p. 713-735.

25. Cai, H. and D.G. Harrison, *Endothelial dysfunction in cardiovascular diseases: the role of oxidant stress.* Circ Res, 2000. **87**(10): p. 840-4.

26. Matsubara, K., et al., *Nitric oxide and reactive oxygen species in the pathogenesis of preeclampsia.* Int J Mol Sci, 2015. **16**(3): p. 4600-14.

27. de Champlain, J., et al., *Oxidative stress in hypertension.* Clin Exp Hypertens, 2004. **26**(7-8): p. 593-601.

28. Dennis, J.M. and P.K. Witting, *Protective Role for Antioxidants in Acute Kidney Disease.* Nutrients, 2017. **9**(7).

29. Nguyen Dinh Cat, A., et al., *Angiotensin II, NADPH oxidase, and redox signaling in the vasculature.* Antioxid Redox Signal, 2013. **19**(10): p. 1110-20.

30. Guzik, T.J. and R.M. Touyz, *Oxidative Stress, Inflammation, and Vascular Aging in Hypertension.* Hypertension, 2017. **70**(4): p. 660-667.

31. Drummond, G.R., et al., *Combating oxidative stress in vascular disease: NADPH oxidases as therapeutic targets.* Nat Rev Drug Discov, 2011. **10**(6): p. 453-71.

32. Araujo, M. and C.S. Wilcox, *Oxidative stress in hypertension: role of the kidney.* Antioxid Redox Signal, 2014. **20**(1): p. 74-101.

33. Divakaran, S. and J. Loscalzo, *The Role of Nitroglycerin and Other Nitrogen Oxides in Cardiovascular Therapeutics.* J Am Coll Cardiol, 2017. **70**(19): p. 2393-2410.

34. Katsuki, S., et al., *Stimulation of guanylate cyclase by sodium nitroprusside, nitroglycerin and nitric oxide in various tissue preparations and comparison to the effects of sodium azide and hydroxylamine.* J Cyclic Nucleotide Res, 1977. **3**(1): p. 23-35.

35. Chen, Z., J. Zhang, and J.S. Stamler, *Identification of the enzymatic mechanism of nitroglycerin bioactivation.* Proc Natl Acad Sci U S A, 2002. **99**(12): p. 8306-11.

36. Millar, T.M., et al., *Xanthine oxidoreductase catalyses the reduction of nitrates and nitrite to nitric oxide under hypoxic conditions.* FEBS Lett, 1998. **427**(2): p. 225-8.

37. Li, H., et al., *Xanthine oxidase catalyzes anaerobic transformation of organic nitrates to nitric oxide and nitrosothiols: characterization of this mechanism and the link between organic nitrate and guanylyl cyclase activation.* J Biol Chem, 2005. **280**(17): p. 16594-600.

38. Munzel, T., S. Steven, and A. Daiber, *Organic nitrates: update on mechanisms underlying vasodilation, tolerance and endothelial dysfunction.* Vascul Pharmacol, 2014. **63**(3): p. 105-13.

39. Daiber, A. and T. Munzel, *Organic Nitrate Therapy, Nitrate Tolerance, and Nitrate-Induced Endothelial Dysfunction: Emphasis on Redox Biology and Oxidative Stress.* Antioxid Redox Signal, 2015. **23**(11): p. 899-942.

40. Lundberg, J.O., M.T. Gladwin, and E. Weitzberg, *Strategies to increase nitric oxide signalling in cardiovascular disease.* Nat Rev Drug Discov, 2015. **14**(9): p. 623-41.

41. Kelm, M., *Nitric oxide metabolism and breakdown.* Biochim Biophys Acta, 1999. **1411**(2-3): p. 273-89.

42. Weitzberg, E. and J.O. Lundberg, *Novel aspects of dietary nitrate and human health.* Annu Rev Nutr, 2013. **33**: p. 129-59.

43. Lundberg, J.O., E. Weitzberg, and M.T. Gladwin, *The nitrate-nitrite-nitric oxide pathway in physiology and therapeutics.* Nat Rev Drug Discov, 2008. **7**(2): p. 156-67.

44. Lundberg, J.O. and E. Weitzberg, *NO generation from nitrite and its role in vascular control.* Arterioscler Thromb Vasc Biol, 2005. **25**(5): p. 915-22.

45. Brkic, D., et al., *Nitrate in Leafy Green Vegetables and Estimated Intake.* Afr J Tradit Complement Altern Med, 2017. **14**(3): p. 31-41.

46. van Velzen, A.G., et al., *The oral bioavailability of nitrate from nitrate-rich vegetables in humans.* Toxicol Lett, 2008. **181**(3): p. 177-81.

47. Lundberg, J.O. and M. Govoni, *Inorganic nitrate is a possible source for systemic*

generation of nitric oxide. Free Radic Biol Med, 2004. **37**(3): p. 395-400.

48. Hezel, M.P. and E. Weitzberg, *The oral microbiome and nitric oxide homoeostasis.* Oral Dis, 2015. **21**(1): p. 7-16.

49. Lundberg, J.O. and E. Weitzberg, *Biology of nitrogen oxides in the gastrointestinal tract.* Gut, 2013. **62**(4): p. 616-29.

50. Cantu-Medellin, N. and E.E. Kelley, *Xanthine oxidoreductase-catalyzed reduction of nitrite to nitric oxide: insights regarding where, when and how.* Nitric Oxide, 2013. **34**: p. 19-26.

51. Bortolotti, M., et al., *Xanthine oxidoreductase: One enzyme for multiple physiological tasks.* Redox Biol, 2021. **41**: p. 101882.

52. Jensen, F.B., *The role of nitrite in nitric oxide homeostasis: a comparative perspective.* Biochim Biophys Acta, 2009. **1787**(7): p. 841-8.

53. Salgado, M.T., E. Nagababu, and J.M. Rifkind, *Quantification of intermediates formed during the reduction of nitrite by deoxyhemoglobin.* J Biol Chem, 2009. **284**(19): p. 12710-8.

54. Shiva, S., et al., *Deoxymyoglobin is a nitrite reductase that generates nitric oxide and regulates mitochondrial respiration.* Circ Res, 2007. **100**(5): p. 654-61.

55. Maia, L.B., et al., *Nitrite reductase activity of rat and human xanthine oxidase, xanthine dehydrogenase, and aldehyde oxidase: evaluation of their contribution to NO formation in vivo.* Biochemistry, 2015. **54**(3): p. 685-710.

56. Cortes-Puch, I., et al., *Inhaled nebulized nitrite and nitrate therapy in a canine model of hypoxia-induced pulmonary hypertension.* Nitric Oxide, 2019. **91**: p. 1-14.

57. Waltz, P., et al., *Nitrate/Nitrite as Critical Mediators to Limit Oxidative Injury and Inflammation.* Antioxid Redox Signal, 2015. **23**(4): p. 328-39.

58. Zhang, G., et al., *Renovascular effects of inorganic nitrate following ischemia-reperfusion of the kidney.* Redox Biol, 2021. **39**: p. 101836.

59. Ashor, A.W., J. Lara, and M. Siervo, *Medium-term effects of dietary nitrate supplementation on systolic and diastolic blood pressure in adults: a systematic review and meta-analysis.* J Hypertens, 2017. **35**(7): p. 1353-1359.

60. Shiva, S., et al., *Nitrite augments tolerance to ischemia/reperfusion injury via the modulation of mitochondrial electron transfer.* J Exp Med, 2007. **204**(9): p. 2089-102.

61. Bryan, N.S., et al., *Dietary nitrite supplementation protects against myocardial ischemia-reperfusion injury.* Proc Natl Acad Sci U S A, 2007. **104**(48): p. 19144-9.

62. Lundberg, J.O., M. Carlstrom, and E. Weitzberg, *Metabolic Effects of Dietary Nitrate in Health and Disease.* Cell Metab, 2018. **28**(1): p. 9-22.

63. Yang, T., et al., *Dietary nitrate attenuates renal ischemia-reperfusion injuries by*

modulation of immune responses and reduction of oxidative stress. Redox Biol, 2017. **13**: p. 320-330.

64.   Carlstrom, M., et al., *Microbiota, diet and the generation of reactive nitrogen compounds.* Free Radic Biol Med, 2020. **161**: p. 321-325.

65.   Norouzirad, R., et al., *Dietary inorganic nitrate attenuates hyperoxia-induced oxidative stress in obese type 2 diabetic male rats.* Life Sci, 2019. **230**: p. 188-196.

66.   Li, S., et al., *Dietary Inorganic Nitrate Protects Hepatic Ischemia-Reperfusion Injury Through NRF2-Mediated Antioxidative Stress.* Front Pharmacol, 2021. **12**: p. 634115.

67.   Schiffer, T.A., et al., *Modulation of mitochondria and NADPH oxidase function by the nitrate-nitrite-NO pathway in metabolic disease with focus on type 2 diabetes.* Biochim Biophys Acta Mol Basis Dis, 2020. **1866**(8): p. 165811.

68.   Kleinbongard, P., et al., *Red blood cells express a functional endothelial nitric oxide synthase.* Blood, 2006. **107**(7): p. 2943-51.

69.   Grau, M., et al., *High red blood cell nitric oxide synthase activation is not associated with improved vascular function and red blood cell deformability in sickle cell anaemia.* Br J Haematol, 2015. **168**(5): p. 728-36.

70.   Yang, J., et al., *Arginase regulates red blood cell nitric oxide synthase and export of cardioprotective nitric oxide bioactivity.* Proc Natl Acad Sci U S A, 2013. **110**(37): p. 15049-54.

71.   Suvorava, T. and M.M. Cortese-Krott, *Exercise-Induced Cardioprotection via eNOS: A Putative Role of Red Blood Cell Signaling.* Curr Med Chem, 2018. **25**(34): p. 4457-4474.

72.   Ozuyaman, B., et al., *RBC NOS: regulatory mechanisms and therapeutic aspects.* Trends Mol Med, 2008. **14**(7): p. 314-22.

73.   Nagarajan, S., et al., *Mechanical perturbations trigger endothelial nitric oxide synthase activity in human red blood cells.* Sci Rep, 2016. **6**: p. 26935.

74.   Baskurt, O.K., P. Ulker, and H.J. Meiselman, *Nitric oxide, erythrocytes and exercise.* Clin Hemorheol Microcirc, 2011. **49**(1-4): p. 175-81.

75.   Leo, F., et al., *Red Blood Cell and Endothelial eNOS Independently Regulate Circulating Nitric Oxide Metabolites and Blood Pressure.* Circulation, 2021. **144**(11): p. 870-889.

76.   Yang, J., et al., *Red Blood Cells in Type 2 Diabetes Impair Cardiac Post-Ischemic Recovery Through an Arginase-Dependent Modulation of Nitric Oxide Synthase and Reactive Oxygen Species.* JACC Basic Transl Sci, 2018. **3**(4): p. 450-463.

77.   Zhou, Z., et al., *Erythrocytes From Patients With Type 2 Diabetes Induce Endothelial Dysfunction Via Arginase I.* J Am Coll Cardiol, 2018. **72**(7): p. 769-780.

78.   Mahdi, A., et al., *Red Blood Cell Peroxynitrite Causes Endothelial Dysfunction in Type*

2 Diabetes Mellitus via Arginase. Cells, 2020. **9**(7).

79. McCann Haworth, S.M., et al., *Red blood cells from patients with pre-eclampsia induce endothelial dysfunction.* J Hypertens, 2021.

80. Gao, X., et al., *NADPH oxidase in the renal microvasculature is a primary target for blood pressure-lowering effects by inorganic nitrate and nitrite.* Hypertension, 2015. **65**(1): p. 161-70.

81. Hezel, M., et al., *Dietary nitrate improves age-related hypertension and metabolic abnormalities in rats via modulation of angiotensin II receptor signaling and inhibition of superoxide generation.* Free Radic Biol Med, 2016. **99**: p. 87-98.

82. Carlstrom, M., et al., *Role of NOX2 in the regulation of afferent arteriole responsiveness.* Am J Physiol Regul Integr Comp Physiol, 2009. **296**(1): p. R72-9.

83. Lai, E.Y., et al., *p47(phox) is required for afferent arteriolar contractile responses to angiotensin II and perfusion pressure in mice.* Hypertension, 2012. **59**(2): p. 415-20.

84. Lai, E.Y., et al., *Norepinephrine increases calcium sensitivity of mouse afferent arteriole, thereby enhancing angiotensin II-mediated vasoconstriction.* Kidney Int, 2009. **76**(9): p. 953-9.

85. Montenegro, M.F., et al., *Profound differences between humans and rodents in the ability to concentrate salivary nitrate: Implications for translational research.* Redox Biol, 2016. **10**: p. 206-210.

86. Li, H., et al., *Characterization of the magnitude and kinetics of xanthine oxidase-catalyzed nitrate reduction: evaluation of its role in nitrite and nitric oxide generation in anoxic tissues.* Biochemistry, 2003. **42**(4): p. 1150-9.

87. Munzel, T., A. Daiber, and A. Mulsch, *Explaining the phenomenon of nitrate tolerance.* Circ Res, 2005. **97**(7): p. 618-28.

88. Omar, S.A., E. Artime, and A.J. Webb, *A comparison of organic and inorganic nitrates/nitrites.* Nitric Oxide, 2012. **26**(4): p. 229-40.

89. Peleli, M., et al., *Renal denervation attenuates hypertension and renal dysfunction in a model of cardiovascular and renal disease, which is associated with reduced NADPH and xanthine oxidase activity.* Redox Biol, 2017. **13**: p. 522-527.

90. Damacena-Angelis, C., et al., *Nitrate decreases xanthine oxidoreductase-mediated nitrite reductase activity and attenuates vascular and blood pressure responses to nitrite.* Redox Biol, 2017. **12**: p. 291-299.

91. Cordero-Herrera, I., et al., *AMP-activated protein kinase activation and NADPH oxidase inhibition by inorganic nitrate and nitrite prevent liver steatosis.* Proc Natl Acad Sci U S A, 2019. **116**(1): p. 217-226.

92. Kelly, J.T., et al., *Modifiable Lifestyle Factors for Primary Prevention of CKD: A Systematic Review and Meta-Analysis.* J Am Soc Nephrol, 2021. **32**(1): p. 239-253.